Averaged Relative Motion and Applications to Formation Flight Near Perturbed Orbits

Prasenjit Sengupta*, Srinivas R. Vadali† and Kyle T. Alfriend‡
Texas A&M University, College Station, TX 77843-3141

Abstract

This paper presents expressions for describing averaged relative motion between two satellites in neighboring orbits about an oblate planet. The theory assumes small relative distances between the satellites, but is uniformly valid for all elliptic orbits as well the special case of a circular reference orbit, by the use of nonsingular orbital elements. These expressions are useful when the short-periodic variations in relative position and velocity are of limited interest, and instead the time-averaged behavior of the states is sought. The averaged expressions also provide insight into the effects of an oblate planet on bounded relative motion. For example, a bias term due to oblateness effects, hitherto unreported, has been identified in the radial position, which can be accounted for in the reference trajectory. Application of these expressions are shown in the derivation of an analytical filter that removes short-periodic variations in relative states, without the use of tuned numerical filters, one for each frequency of interest, which are normally used for disturbance accommodation in control system design. The use of this analytical filter is demonstrated for formation-keeping on a prescribed relative trajectory.

*Research Associate, Department of Aerospace Engineering, MS 3141, prasenjit@tamu.edu, Member, AIAA.

†Stewart & Stevenson - I Professor, Department of Aerospace Engineering, MS 3141, svadali@aero.tamu.edu, Associate Fellow, AIAA.

‡TEES Distinguished Research Chair Professor, Department of Aerospace Engineering, MS 3141, alfriend@aero.tamu.edu, Fellow, AIAA.

Nomenclature

a	= semimajor axis
e	= eccentricity
(E, f)	= eccentric and true anomalies
g	= argument of perigee
h	= right ascension
J_2	= second zonal harmonic coefficient of the Earth's gravity field
i	= inclination
l	= mean anomaly
$(\dot{l}_s, \dot{g}_s, \dot{h}_s)$	= secular rates of (l, g, h)
(L, G, H)	= conjugate momenta, Delaunay elements
n	= satellite mean motion
$\boldsymbol{\text{œ}}$	= orbital element vector
(q_1, q_2)	= nonsingular variables ($e\cos g$, $e\sin g$)
r	= radial distance of the satellite
$R_\oplus$	= Earth radius
(v_r, v_θ, v_h)	= satellite velocity components, rotating Cartesian frame (radial, along-track, out-of-plane)
(x, y, z)	= scaled relative position coordinates (radial, along-track, out-of-plane)
$\mathbf{x}$	= relative state vector
$\boldsymbol{\delta\text{œ}}$	= differential orbital element vector
Δt	= elapsed time since epoch
(λ, θ)	= mean and true arguments of latitude
μ	= gravitational coefficient
ϕ	= latitude of the satellite
$(\omega_r, \omega_\theta, \omega_h)$	= angular velocity components of the rotating Cartesian frame (radial, along-track, out-of-plane)
(ξ, ϑ, η)	= relative position coordinates (radial, along-track, out-of-plane)
$(\bar{\ })$	= function obtained using mean elements
$(\widehat{\ })$	= average of a function of osculating elements
$(\dot{\ })$	= derivative with respect to time
$(')$	= derivative with respect to mean anomaly

Introduction

Formation flight is an emerging technology where several satellites are placed in proximity to each other, for various purposes, such as terrestrial observation, communication,

and stellar interferometry. Typically, relative motion between satellites is described with respect to a 'chief' satellite (also called the 'leader' or 'target'), which could be real or virtual. The dynamics of the other satellites (called the 'deputies', 'followers', or 'chasers') are expressed either in a Cartesian, Local-Vertical-Local Horizontal (LVLH) frame, rotating with the chief, or by using the satellites' orbital element differences. The simplest equations modeling relative motion dynamics were derived by Hill[1], and used by Clohessy and Wiltshire[2] to study the rendezvous problem; these equations are collectively known as the Hill-Clohessy-Wiltshire model. This model assumes small relative distances (linearized differential gravity), a circular reference orbit, and a central gravitation field. Several works in the literature study the problem of relative motion when one or more of the underlying assumptions are violated. For example, the linear, eccentric problem was solved independently by Lawden[3] and Tschauner and Hempel[4], and several elegant solutions to this model exist[5]. A state transition matrix for relative motion near eccentric orbits that included perturbing oblateness effects was derived by Gim and Alfriend[6]. Their work used nonsingular elements for uniform validity of the theory for the circular case, and was extended in [7], using equinoctial elements, for singularities associated with the equatorial case. Work by Kasdin *et al.*[8] used Hamilton-Jacobi theory to develop relative motion expressions near circular orbits that included nonlinearity and perturbation effects. Perturbation equations for satellite motion, and satellite relative motion, were developed by Gurfil[9], by using gauge-generalized variation-of-parameter equations for the orbital elements. These equations were used to identify perturbation-invariant orbits. Nonlinear, perturbed relative motion near eccentric orbits has been studied by Alfriend *et al.*[10], and Sengupta *et al.*[11]. Reference [11] also derived state transition matrices and tensors that are accurate for large relative orbits.

Of interest in this paper, is the averaged behavior of a satellite in a relative orbit near another. In other words, expressions are desired that average the short-periodic variations induced by oblateness effects, and instead only describe the time-averaged behavior of the relative states. These expressions are useful in providing a general idea of how the relative states propagate in time. Furthermore, they are also useful in the design of control laws where the periodic behavior is of limited interest, and where control laws that do not respond to such behavior are desirable, thereby leading to increased fuel saving. Examples of such control laws were derived by Vadali *et al.*[12]. In their work, tuned filters obtained via numerical integration were used. In this paper, it is shown how the theory of averaged relative motion can be successfully used to design such filters analytically.

A mean orbital element description was also used by Schaub and Alfriend[13] to design J_2-invariant orbits. Although a transformation matrix using mean elements, between differential mean elements, and the states, was derived in [6], this does not result in averaged

relative motion, that is, the states obtained from this transformation are not the same as those obtained by averaging osculating element-based relative motion with respect to time. This is because the mean elements are the result of the doubly-averaged Hamiltonian, and the averaging process removes periodic terms. In reality, the averaging process should be performed as a final step, which allows for the inclusion of the non-zero-average product of two zero-average terms (a trivial example is the product of two sine curves of the same frequency, which has an average value of 1/2 over one period, although the individual sine curves themselves have a zero average).

This paper uses an orbital element approach, as previously followed by several authors[6, 14, 15]. Consequently, relative motion is examined in the linear sense, but with oblateness effects due to J_2 accounted for. The paper is organized as follows: the effects of J_2 on a satellite's orbit, and on satellite relative motion, are presented. The procedure of deriving the average value of a function due to oblateness effects is then presented, and it is shown how this is different from the mean function. The averaged expressions for relative motion are developed, and although the complete results are presented as an appendix, the particular case of relative motion near a circular orbit is analyzed. The averaged relative motion expressions allow for the identification of bias and growth terms. A J_2-induced bias in the radial position is identified, that cannot be obtained if a mean element model is used. These results are then used to design a filter for J_2 perturbations, and the use of this filter is demonstrated on a formation-keeping problem. All developments are supported by numerical examples.

Oblateness Effects on Orbital Motion and Relative Motion

The orbit of any satellite is completely determined by the six elements a, e, i, h, g, and l. In the two-body problem, the first five quantities are constants, and the mean anomaly is a linear function of time, given by $l = l_0 + n\,\Delta t$, where l_0 is the mean anomaly at epoch, and $n = \sqrt{\mu/a^3}$. In the presence of perturbations or control acceleration, the orbital elements are no longer constant, and their rates can be obtained using Gauss' equations[16]. The satellite's orbital radius r is obtained from f, which is dependent on l through its relation to E, and Kepler's equation relating E to l [16]:

$$\tan\frac{f}{2} = \sqrt{\frac{1+e}{1-e}}\tan\frac{E}{2} \tag{1}$$

$$l = E - e\sin E \tag{2}$$

To avoid zero-eccentricity singularities associated with the classical orbital element set, this paper uses a nonsingular element set, given by $\mathbf{oe} = \{a\ \lambda\ i\ q_1\ q_2\ h\}^\top$, where $\lambda = g + l$.

Similarly, the true argument of latitude is defined as $\theta = g + f$. The use of nonsingular elements is essential for solutions that are uniformly valid for $0 \leq e < 1$. However, their use does not avoid singularities introduced by equatorial or near-equatorial orbits ($i \sim 0$); these cases can be analyzed using nonsingular equinoctial elements[17] and are beyond the scope of this paper.

A full development of the theory of oblateness effects on satellite motion is presented in [18]. For Earth operations, it is sufficient to extend the development to the first zonal harmonic term (due to the equatorial bulge), which has a coefficient $J_2 = 1.08269 \times 10^{-3}$, since the terms contributed by higher-order zonal, tesseral, and sectorial harmonics, are three magnitudes smaller. Consequently, the gravitational potential, $\mathcal{V}$, including oblateness effects is modeled as follows:

$$\mathcal{V}(r, \phi) = -\frac{\mu}{r}\left[1 + J_2\left(\frac{R_\oplus}{r}\right)^2 P_2\left(\sin\phi\right)\right] \tag{3}$$

where P_2 is the second Legendre polynomial.

The effects on the orbital elements, to the first order in J_2, have been studied by Brouwer[19] and Kozai[20], and are classified as secular growth, short-periodic, and long-periodic perturbations. If the study of the change of orbital elements is limited to that due to the first-order secular component, it can be shown that orbital elements a, e, and i can be considered constant, and the elements l, g, and h depart linearly from their initial values l_0, g_0, and h_0, respectively. These elements are known as mean elements, and will henceforth be denoted by an overbar (for example, $\bar{a}$ denotes the mean semimajor axis). The secular rates of l, g, and h, are given by:

$$\dot{l}_s = \sqrt{\frac{\mu}{\bar{a}^3}}\left[1 - \frac{3}{4}\bar{\eta}J_2\left(\frac{R_\oplus}{\bar{a}\bar{\eta}^2}\right)^2\left(1 - 3\cos^2\bar{i}\right)\right] \tag{4a}$$

$$\dot{g}_s = -\frac{3}{4}\sqrt{\frac{\mu}{\bar{a}^3}}J_2\left(\frac{R_\oplus}{\bar{a}\bar{\eta}^2}\right)^2\left(1 - 5\cos^2\bar{i}\right) \tag{4b}$$

$$\dot{h}_s = -\frac{3}{2}\sqrt{\frac{\mu}{\bar{a}^3}}J_2\left(\frac{R_\oplus}{\bar{a}\bar{\eta}^2}\right)^2\cos\bar{i} \tag{4c}$$

where $\eta = \sqrt{1 - e^2}$. As a consequence, the mean nonsingular elements $\bar{\lambda}$, $\bar{q}_1$, and $\bar{q}_2$ have the following mean variations:

$$\bar{\lambda} = \bar{\lambda}_0 + \dot{\lambda}_s\,\Delta t = \bar{\lambda}_0 + \left(\dot{l}_s + \dot{g}_s\right)\Delta t \tag{5a}$$

$$\bar{q}_1 = \bar{q}_{10}\cos\left(\dot{g}_s\,\Delta t\right) - \bar{q}_{20}\sin\left(\dot{g}_s\,\Delta t\right) \tag{5b}$$

$$\bar{q}_2 = \bar{q}_{10} \sin(\dot{g}_s \, \Delta t) + \bar{q}_{20} \cos(\dot{g}_s \, \Delta t) \tag{5c}$$

where $\bar{q}_{10} + \jmath \, \bar{q}_{20} = \bar{e} \, \exp(\jmath \bar{g}_0)$, and $\jmath = \sqrt{-1}$. If the short-periodic and long-periodic perturbations are also included then the instantaneous elements, also known as osculating elements, describe the true orbit.

While [19] posed the problem of orbital element variation as a solution to a Hamiltonian system, with J_2 as a perturbation parameter, [20] obtained the secular, short- and long-periodic behavior by a process of averaging. Furthermore, [19] derived generating functions for the short- and long-periodic variations, to the second-order in J_2, by the use of (canonical) Delaunay elements, that are given by the sets ($L = \sqrt{a}$, $G = L\eta$, $H = G \cos i$), and (l, g, h). The osculating elements can therefore be obtained from the mean elements by the addition of periodic variations that are also dependent on mean elements.

The Delaunay elements L and G are identical when the orbit is circular, and the Brouwer transformation loses validity for $e < 0.05$, due to the presence of singularities in the resulting solutions. This problem has been dealt with using a variety of techniques. Smith[21] reformulated the problem in terms of inertial coordinates without the singular terms, and analytically determined the required correction to these coordinates. Kozai[22] extended the results of [20] by using q_1, $-q_2$, and λ, instead of the elements e, g and l. Brouwer's theory has also been modified by the use of other canonical variable sets, such as the Poincaré variables[23], or Hill's variables[24]. Hoots[25] used a set of 'position elements', that are valid for the circular and/or equatorial case. However, the exact formulation used is not important. As shown in [6, 7], the short- and long-periodic variations in nonsingular or equinoctial elements can also be obtained by using the generating functions in [19], since the partials of these variables with respect to the Delaunay elements are known. Consequently, this paper will only refer to the transformation from mean to osculating elements as Brouwer theory, irrespective of the element set used.

This paper limits results accurate to the first order in J_2 only, since an inclusion of second order terms is meaningless without the inclusion of tesseral and sectorial harmonics and higher-order zonal harmonics in the potential. However, other works in the literature do extend analysis to $\mathcal{O}(J_2^2)$ and higher. For example, [26] obtained analytical expressions for short- and long-periodic variations through $\mathcal{O}(J_2^3)$, and for secular variations through $\mathcal{O}(J_2^4)$. In their work, eccentricity expansions were made use of, limiting usage to near-circular orbits. This was corrected by Aksnes[27], who provided the solutions to several integrals used in [26], without the assumption of small eccentricity. References [28, 29] used symbolic algebra to extend the theory to the third and fourth order, respectively, valid for $0 \leq e < 1$.

The effects of J_2 on formation flight manifest themselves through differential relative

acceleration terms, and by a precession of the rotating frame. The short-periodic variations in a, e, and i also have an effect on relative motion. The complete nonlinear description in the presence of J_2 perturbations has been developed by Kechichian[30], although the system of equations presented therein cannot be solved in closed form. Simplified, linear relative motion models that include J_2 effects were developed by Vadali *et al.*[12] and Schweigart and Sedwick[31], but their use is limited to circular reference orbits and small relative orbits only. The state transition matrix (STM) formulated by Gim and Alfriend[6], using the geometric method in nonsingular orbital elements, also accounts for first-order J_2 effects. This STM can completely characterize linear relative motion in eccentric orbits. A similar result was obtained by Yan *et al.*[32], but by utilizing the unit sphere formulation for relative motion[33].

Averaged Functions of the Orbital Elements

In this section, the process of averaging a function of the osculating orbital elements is discussed. The concept of an averaged function is first presented. This concept is then applied to relative motion perturbed by J_2, since relative position and velocity can be written as functions of the chief's orbital elements and differential orbital elements.

Averaged Functions and Mean Functions

To understand the development and use of expressions for averaged relative motion, it is first necessary to distinguish between the time-average of a function of the Delaunay elements, and a function of the mean Delaunay elements. If $\mathbf{oe}$ is any osculating element set describing an orbit, then it can be obtained from the corresponding mean elements $\overline{\mathbf{oe}}$ by using a first-order transformation presented in [19]. Let $\kappa(\mathbf{oe})$ be any function of the orbital elements. Then the following hold:

$$\overline{\kappa}(\mathbf{oe}) \triangleq \kappa(\overline{\mathbf{oe}}) \tag{6a}$$

$$\widehat{\kappa}(\mathbf{oe}) \neq \kappa(\overline{\mathbf{oe}}) \tag{6b}$$

Eqs. (6a) and Eq. (6b) imply that although the mean function $\overline{\kappa}$ is obtained by substituting mean elements in the function κ, this is not the same as the time-averaged function $\widehat{\kappa}$. Since Eq. (6a) is simply obtained by substituting mean elements in place of the corresponding osculating elements, it is easier to calculate, but physically less meaningful than Eq. (6b). As shown by Brouwer[19], if the potential due J_2 is treated as a perturbation to the two-body Hamiltonian in the Delaunay elements, then a series of canonical transformations result in the mean elements, of which $\overline{L}$, $\overline{G}$, and $\overline{H}$ are constants, and $\bar{l}$, $\bar{g}$, and $\bar{h}$ are linear functions of time, whose rates are given by Eqs. (4). The inverse transformation used to obtain short- and

long-periodic variations, is derived by the use of generating functions that are also functions of the mean elements. Consequently, the osculating elements can be obtained as a function of the mean elements. The mean elements, and the long-periodic elements are also referred to as doubly- and singly-averaged elements, respectively, by virtue of the fact that they result from the doubly- and singly-averaged Hamiltonian.

A function κ of the osculating elements, can be obtained to $\mathcal{O}(J_2)$ as follows:

$$\kappa(\mathbf{oe}) = \kappa(\overline{\mathbf{oe}}) + \kappa_{\text{sp}}(\overline{\mathbf{oe}}) + \kappa_{\text{lp}}(\overline{\mathbf{oe}}) \tag{7}$$

where κ_{sp} and κ_{lp} are the short-periodic and long-periodic variations in κ, respectively. For a limited number of orbits, where the time of operation considered is significantly less than the period of perigee drift, long-periodic perturbations exhibit themselves as secular growth of $\mathcal{O}(J_2^2)$, and are therefore neglected in this paper. Consequently, the average value of the function, which accounts for the averaged J_2 variation in the function, is given by:

$$\widehat{\kappa}(\mathbf{oe}) = \kappa(\overline{\mathbf{oe}}) + \frac{1}{2\pi}\int_0^{2\pi} \kappa_{\text{sp}}(\overline{\mathbf{oe}})\, dl \tag{8}$$

In Eq. (8), the mean anomaly is selected as the variable of integration since it is proportional to time. The choice of l over $\bar{l}$ as the variable of integration is irrelevant since $\kappa_{\text{sp}} = \mathcal{O}(J_2)$. The short-periodic variation, κ_{sp}, is obtained as follows:

$$\kappa_{\text{sp}}(\overline{\mathbf{oe}}) = -J_2 R_\oplus^2 \left(\bar{\kappa}, W_{\text{sp}_1} + W_{\text{sp}_2}\right) \tag{9}$$

where $(\cdot,\cdot)$ denotes the Poisson bracket operator, and W_{sp_1} and W_{sp_2} are the short-periodic generating functions, as shown in [19]:

$$W_{\text{sp}_1} = -\frac{1}{4\overline{G}^3}\left(1 - 3\frac{\overline{H}^2}{\overline{G}^2}\right)\left(\bar{f} - \bar{l} + \bar{e}\sin\bar{f}\right) \tag{10a}$$

$$W_{\text{sp}_2} = \frac{3}{8\overline{G}^3}\left(1 - \frac{\overline{H}^2}{\overline{G}^2}\right)\left[\sin(2\bar{f} + 2\bar{g}) + \bar{e}\sin(\bar{f} + 2\bar{g}) + \frac{\bar{e}}{3}\sin(3\bar{f} + 2\bar{g})\right] \tag{10b}$$

Since the classical orbital elements are themselves functions of the canonical elements, the averages of their short-periodic variations is not the same as their respective mean values. The averages of the short-periodic variations in the classical orbital elements are presented in [20]. As shown in [20], the short-periodic terms for the eccentricity, argument of perigee, and mean anomaly cannot be determined when $\bar{e} = 0$, because g cannot be determined independent of f or l. Furthermore, since the osculating eccentricity can never be negative,

the average eccentricity must necessarily be non-zero, even though the mean eccentricity may be zero. The short-periodic formulae for the eccentricity can be shown to result in negative eccentricity, when the mean eccentricity is zero. For these reasons, the nonsingular elements are used.

Averaged Relative Motion

The approach in this section is to first define the relative states in terms of differential osculating elements, and the kinematic states of the chief, given by the radius, velocity components in the LVLH frame, and angular rates of the LVLH frame[34]. These are found to be a more convenient description than the orbital elements themselves. Finally, the functions are averaged using several integrals of the true and mean anomaly.

The relative state vector is composed of the relative position coordinates, (ξ, ϑ, ζ), and relative velocity coordinates, $(\dot{\xi}, \dot{\vartheta}, \dot{\zeta})$. In this paper, a non-dimensional state vector $\mathbf{x} = \{x\ y\ z\ x'\ y'\ z'\}^\top$ is used, where

$$\{x\ y\ z\ x'\ y'\ z'\}^\top = \{\xi/\bar{a}\ \ \vartheta/\bar{a}\ \ \zeta/\bar{a}\ \ \dot{\xi}/(\bar{n}\bar{a})\ \ \dot{\vartheta}/(\bar{n}\bar{a})\ \ \dot{\zeta}/(\bar{n}\bar{a})\}^\top \tag{11}$$

The relative position is scaled by the mean semimajor axis of the chief, and the relative velocities are scaled by the velocity-like quantity $\bar{n}\bar{a}$, where $\bar{n}$ is the mean motion using mean elements, given by $\sqrt{\mu/\bar{a}^3}$.

Let $\boldsymbol{\delta oe} \triangleq \{\delta a/a\ \delta\lambda\ \delta i\ \delta q_1\ \delta q_2\ \delta h\}^\top$. The differential semimajor axis, δa, is scaled by the chief's semimajor axis, a, to make it dimensionally equivalent to the other components of the vector. The vector $\boldsymbol{\delta\overline{oe}}$ denotes the mean differential orbital elements, which can be propagated using the mean rates. Furthermore, the subscript '0' will be used to denote the value of the respective quantity at epoch. In two-body motion, $\delta q_1 = \delta q_{10}$, $\delta q_2 = \delta q_{20}$, and $\delta h = \delta h_0$; however, in the presence of perturbations, these quantities show secular drift.

A description of the following form is desired:

$$\widehat{\mathbf{x}}(\Delta t) = [\mathbf{P}_0(\overline{\mathbf{oe}}) + J\mathbf{P}_J(\overline{\mathbf{oe}})]\, \boldsymbol{\delta\overline{oe}}(\Delta t) \tag{12}$$

where $J = J_2 R_\oplus^2/(\bar{a}^2\bar{\eta}^4)$, $\mathbf{P}_0(\overline{\mathbf{oe}})$ is the transformation matrix corresponding to the non-J_2 problem, composed of mean elements, and $\mathbf{P}_J(\overline{\mathbf{oe}})$ is a correction that is added to calculate the averaged relative motion (see Appendix C). It should be noted that the averaged states $\widehat{\mathbf{x}}$ are different from the mean states $\overline{\mathbf{x}}$, which would be the states obtained by using transformation matrix for mean elements $\overline{\boldsymbol{\Sigma}}$, derived in [6], in Eq. (12). The advantage of the averaged states as defined in Eq. (12), is that mean elements of the chief, and mean differential orbital elements can be used everywhere, and short-periodic computations may be avoided.

From the geometric description of relative motion[6], it can be shown that:

$$\xi = \delta r \tag{13a}$$
$$\vartheta = r(\delta\theta + \delta h\, \cos i) \tag{13b}$$
$$\zeta = r(\delta i\, \sin\theta - \delta h\, \sin i\, \cos\theta) \tag{13c}$$
$$\dot{\xi} = \delta v_r \tag{13d}$$
$$\dot{\vartheta} = \delta v_\theta + v_r(\delta\theta + \delta h\, \cos i) - v_h(\delta i\, \cos\theta + \delta h\, \sin i\, \sin\theta) - \omega_h\, \xi + \omega_r\, \zeta \tag{13e}$$
$$\dot{\zeta} = \delta v_h + v_r(\delta i\, \sin\theta - \delta h\, \sin i\, \cos\theta) + v_\theta(\delta i\, \cos\theta + \delta h\, \sin i\, \sin\theta) - \omega_r\, \vartheta + \omega_\theta\, \xi \tag{13f}$$

For the sake of brevity, the functions α and β are used throughout the paper, that are defined as follows:

$$\alpha + \jmath\beta \triangleq 1 + (q_1 - \jmath q_2)\, \exp(\jmath\theta) \tag{14}$$

Similarly, $\bar{\alpha}$ and $\bar{\beta}$ refer to the calculation of Eq. (14) using mean elements. It is easily shown that:

$$\frac{\partial\alpha}{\partial\theta} = -\beta, \quad \frac{\partial\alpha}{\partial q_1} = \cos\theta, \quad \frac{\partial\alpha}{\partial q_2} = \sin\theta \tag{15a}$$
$$\frac{\partial\beta}{\partial\theta} = \alpha - 1, \quad \frac{\partial\beta}{\partial q_1} = \sin\theta, \quad \frac{\partial\beta}{\partial q_2} = -\cos\theta \tag{15b}$$

By using Eq. (14), and from [30], it can be shown that:

$$r = \frac{a\eta^2}{\alpha} \tag{16a}$$
$$\omega_r = \dot{h}\sin i \sin\theta + \dot{i}\cos\theta \tag{16b}$$
$$\omega_\theta = \dot{h}\sin i \cos\theta - \dot{i}\sin\theta \tag{16c}$$
$$\omega_h = \frac{n\alpha^2}{\eta^3} \tag{16d}$$
$$v_r = \frac{na\beta}{\eta} \tag{16e}$$
$$v_\theta = r\omega_h = \frac{na\alpha}{\eta} \tag{16f}$$
$$v_h = -r\omega_\theta \tag{16g}$$

It is well known that ω_θ, when evaluated using osculating elements, is always zero[34]. However, if mean elements and secular rates are used to evaluate ω_θ from Eq. (16c), then

$\omega_\theta = \mathcal{O}(J_2)$. Furthermore, $\omega_r = 0$ in the absence of perturbations, and $\omega_r = \mathcal{O}(J_2)$ in the presence of oblateness effects, since $\dot{h}$ and $\dot{i}$ are $\mathcal{O}(J_2)$ in Eq. (16b) . Consequently, both ω_r and ω_θ can be evaluated using mean elements and secular rates, since the inclusion of short- and long-periodic effects of J_2 will only result in contributions of $\mathcal{O}(J_2^2)$. The other quantities may be expressed as the sum of a function using direct substitution of mean elements, and short-periodic variations using the generating functions. For example,

$$r = \bar{r} + J r_{\text{sp}} \tag{17a}$$

$$\text{where,} \quad \bar{r} = \frac{\bar{a}\,\bar{\eta}^2}{\bar{\alpha}} \tag{17b}$$

$$\text{and,} \quad r_{\text{sp}} = -\bar{a}^2\,\overline{\eta}^4\left(\bar{r}, W_{\text{sp}_1} + W_{\text{sp}_2}\right) \tag{17c}$$

After some algebra, the following expressions are obtained for the variables of interest:

$$r_{\text{sp}} = \bar{a}\,\bar{\eta}^2(1-3\cos^2\bar{i})\left(\frac{\bar{\eta}+\bar{\alpha}}{4(1+\bar{\eta})}+\frac{\bar{\eta}}{2\bar{\alpha}}\right)+\frac{\bar{a}\bar{\eta}^2}{4}\sin^2\bar{i}\,\cos 2\overline{\theta} \tag{18a}$$

$$\begin{aligned} w_{h_{\text{sp}}} &= \frac{1}{2}\bar{n}\,(1-3\cos\bar{i}^2)\bar{\alpha}^2\frac{[\bar{\alpha}^2+\bar{\eta}\bar{\alpha}+2\bar{\eta}(1+\bar{\eta})]}{\bar{\eta}^3(1+\bar{\eta})} \\ &\quad +\frac{1}{4\bar{\eta}^3}\bar{n}\sin^2\bar{i}\,\bar{\alpha}^2(\cos 2\overline{\theta}+2\bar{q}_1\cos\overline{\theta}-2\bar{q}_2\sin\overline{\theta}) \end{aligned} \tag{18b}$$

$$v_{r_{\text{sp}}} = -\frac{\bar{a}\,\bar{n}}{4\bar{\eta}(1+\bar{\eta})}(1-3\cos^2\bar{i})\bar{\beta}(\bar{\alpha}^2+\bar{\eta}+\bar{\eta}^2)-\frac{\bar{a}\,\bar{n}}{2\bar{\eta}}\sin^2\bar{i}\,\bar{\alpha}^2\sin 2\overline{\theta} \tag{18c}$$

$$\begin{aligned} v_{\theta_{\text{sp}}} &= -\frac{\bar{a}\,\bar{n}}{4\bar{\eta}(1+\bar{\eta})}(1-3\cos^2\bar{i})\bar{\alpha}\,[\bar{\alpha}(\bar{\eta}+\bar{\alpha})+2\bar{\eta}(1+\bar{\eta})] \\ &\quad +\frac{\bar{a}\,\bar{n}}{4\bar{\eta}}\sin^2\bar{i}\,\left[\bar{\alpha}(1+\bar{\alpha})\cos 2\overline{\theta}+2\bar{\alpha}(\bar{q}_1\cos\overline{\theta}-\bar{q}_2\sin\overline{\theta})\right] \end{aligned} \tag{18d}$$

$$i_{\text{sp}} = \frac{1}{4}\sin\bar{i}\,\cos\bar{i}\,\left(3\cos 2\overline{\theta}+3\bar{q}_1\cos\overline{\theta}-3\bar{q}_2\sin\overline{\theta}+\bar{q}_1\cos 3\overline{\theta}+\bar{q}_2\sin 3\overline{\theta}\right) \tag{18e}$$

$$\begin{aligned} h_{\text{sp}} &= -\frac{3}{2}\cos\bar{i}\,\left(\overline{\theta}-\bar{\lambda}+\bar{\beta}\right) \\ &\quad +\frac{1}{4}\cos\bar{i}\,\left(3\sin 2\overline{\theta}+3\bar{q}_1\sin\overline{\theta}+3\bar{q}_2\cos\overline{\theta}+\bar{q}_1\sin 3\overline{\theta}-\bar{q}_2\cos 3\overline{\theta}\right) \end{aligned} \tag{18f}$$

$$\begin{aligned} \theta_{\text{sp}} &= \frac{\bar{\beta}}{2}-\frac{3}{4}(1-5\cos^2\bar{i})(\overline{\theta}-\bar{\lambda})-\frac{1}{4}(1-3\cos^2\bar{i})\frac{\bar{\beta}}{(1+\bar{\eta})}(\bar{\alpha}+4\bar{\eta}+5) \\ &\quad -\frac{1}{4}\cos^2\bar{i}\,(\bar{q}_1\sin 3\overline{\theta}-\bar{q}_2\cos 3\overline{\theta})+\frac{1}{8}(1-7\cos^2\bar{i})\sin 2\overline{\theta} \\ &\quad +\frac{1}{4}(2-5\cos^2\bar{i})(\bar{q}_1\sin\overline{\theta}+\bar{q}_2\cos\overline{\theta}) \end{aligned} \tag{18g}$$

Two points are noted here. First, $v_{r_{\text{sp}}} \neq \dot{r}_{\text{sp}}$. Second, expressions for short-periodic variations in r have appeared in other works. For example, Kozai[20] obtained a similar expression as shown above; however, numerical computations show that the expression in that reference is

incorrect since it fails to remove a bias. The use of Hill's variables by Aksnes[24] also results in expressions for short-periodic behavior of r and $\dot{r}$. Even though the derivation presented by [24] does not have eccentricity terms in the denominator, and is therefore, nonsingular, the relevant expressions are nevertheless written in terms of the classical orbital elements, some of which are indeterminable for circular orbits. The expressions in this paper are written in nonsingular form and use Eq. (14) for a concise representation. A low-eccentricity approximation for the average radius has also been derived by Born *et al.*[35].

The development of expressions for short-periodic variations in r, v_r, and v_θ is essential to obtain simplified, averaged relative position and velocity. The only other alternative is to individually find the average values of the short-periodic variations in all the orbital elements, in their various functional forms, as shown in [6], compose the expressions for the relative states, and maintain terms through $\mathcal{O}(J_2)$.

Some amount of algebra, performed easily via symbolic computation, is required to obtain the averaged relative position and velocity. The steps involve finding the average values of short-periodic variations in functions of the orbital elements, as shown in Eqs. (18), and require the solutions to integrals of the following form:

$$I_{mk} = \frac{1}{2\pi}\int_0^{2\pi} \frac{\exp(\jmath k f)}{(1+e\cos f)^m}\, dl \tag{19a}$$

$$I_0 = \frac{1}{2\pi}\int_0^{2\pi} (f-l)\,\varrho(f)\, dl \tag{19b}$$

where $k, m \in \mathbb{Z}_{\geq 0}$, $\exp(\jmath k f) = \cos kf + \jmath \sin kf$ is the more general placeholder for the cosine and sine functions, and $\varrho(f)$ is a periodic function, even or odd, which is of the form $1/(1+e\cos f)^m$, $\cos f/(1+e\cos f)^m$, or $\sin f/(1+e\cos f)^m$. Integrals of the form as shown in Eq. (19a) occur when the average value of a term comprising the mean radius is required, or when $(1+e\cos f)$ appears in the denominator of a term. Kozai[20] and Hoots[36] presented solutions to I_{mk}, for specific values of m and k. For the derivations in this paper, it is sufficient to obtain expressions for I_{mk} for $m = 0, 1, 2$, although values of k of upto 9 are required, which are not provided by [20, 36]. It can be shown that:

$$\frac{1}{2\pi}\int_0^{2\pi} \frac{\sin kf\, dl}{(1+e\cos f)^m} = 0 \tag{20a}$$

$$\frac{1}{2\pi}\int_0^{2\pi} \frac{\cos kf\, dl}{(1+e\cos f)^2} = \frac{1}{6\eta^4}(-\varepsilon)^k\left[k^3\eta^3 + 6k^2\eta^2 + k\eta(15-4\eta^2) + (15-9\eta^2)\right] \tag{20b}$$

$$\frac{1}{2\pi}\int_0^{2\pi} \frac{\cos kf\, dl}{(1+e\cos f)} = \frac{1}{2\eta^2}(-\varepsilon)^k\left[k^2\eta^2 + 3k\eta + (3-\eta^2)\right] \tag{20c}$$

$$\frac{1}{2\pi}\int_0^{2\pi} \cos kf \, dl = (-\varepsilon)^k \left[k\eta + 1\right] \tag{20d}$$

where,

$$\varepsilon = \sqrt{\frac{1-\eta}{1+\eta}} = \mathcal{O}(e) \tag{21}$$

The general solution for I_{mk} is presented in Appendix A.

Integrals of the form as shown in Eq. (19b) occur when the average of a quantity comprising θ, $\delta\theta$, or δh is required. Déprit and Rom[26] noted that closed-form solutions to the indefinite integral corresponding to Eq. (19b) could not be found, and there was a possibility that such a solution did not exist. Aksnes[27] has shown that this integral does not require evaluation if the motion of one satellite is analyzed, since a complete expansion results in the cancellation of terms composed of this integral. However, in this paper, the expressions of interest are those arising from satellite relative motion, and it was found that no such cancellation occurred. It can be shown that a series solution to the indefinite form of Eq. (19b) exists, and in particular, that $I_0 = 0$, if $\varrho(f)$ is an even function. The details are presented in Appendix II.

As an example consider the averaged radial displacement due to short-periodic perturbations, since $r = \bar{r} + Jr_{\text{sp}}$, it follows that:

$$\xi = \delta\bar{r} + \delta\left(J\, r_{\text{sp}}\right) \tag{22}$$

and consequently,

$$\widehat{\xi} = \delta\bar{r} + \frac{1}{2\pi}\int_0^{2\pi} \delta(J\, r_{\text{sp}})\, dl \tag{23}$$

From Eq. (16a), $\delta\bar{r}$ is easily obtained to the first order in differential orbital elements, as the following:

$$\delta r = \frac{\eta^2}{\alpha}\,\delta a - \left(2q_1 + \frac{\eta^2\cos\theta}{\alpha}\right)\frac{a}{\alpha}\,\delta q_1 - \left(2q_2 + \frac{\eta^2\sin\theta}{\alpha}\right)\frac{a}{\alpha}\,\delta q_2 + \frac{a\eta^2\beta}{\alpha^2}\,\delta\theta \tag{24}$$

In the above expression, $\delta\theta$, is rewritten in terms $\delta\lambda$, δq_1, and δq_2. This is because $\delta\lambda$ is a linear function of time, in the absence of perturbations, or with the use of mean elements, whereas $\delta\theta$ is not. The relation between $\delta\theta$ and δl is developed using the following equation

from [19]:

$$\delta f = \frac{1}{\eta^3}(1+e\cos f)^2\,\delta l + \frac{1}{\eta^2}\sin f\,(2+e\cos f)\,\delta e \tag{25}$$

$$\text{or,}\qquad \delta\theta - \delta g = \frac{1}{\eta^3}(1+e\cos f)^2\,(\delta\lambda - \delta g) + \frac{1}{\eta^2}\sin f\,(2+e\cos f)\,\delta e \tag{26}$$

Substituting $e^2\,\delta g \approx -q_2\,\delta q_1 + q_1\,\delta q_2$, and $e\,\delta e \approx q_1\,\delta q_1 + q_2\,\delta q_2$ in Eq. (26), the relation $\delta\theta = \gamma_1\,\delta\lambda + \gamma_2\,\delta q_1 + \gamma_3\,\delta q_2$ is obtained, where:

$$\gamma_1 \equiv \gamma_1(q_1,q_2,\theta) = \frac{\alpha^2}{\eta^3} \tag{27a}$$

$$\gamma_2 \equiv \gamma_2(q_1,q_2,\theta) = \frac{q_2\alpha^2}{(1+\eta)\eta^3} + \frac{\sin\theta\,\alpha}{\eta^2} + \frac{q_2+\sin\theta}{\eta^2} \tag{27b}$$

$$\gamma_3 \equiv \gamma_3(q_1,q_2,\theta) = -\frac{q_1\alpha^2}{(1+\eta)\eta^3} - \frac{\cos\theta\,\alpha}{\eta^2} - \frac{q_1+\cos\theta}{\eta^2} \tag{27c}$$

The mean orbital element differences can be obtained in terms of their initial values, in a manner similar to that described in [6]. In particular, $\delta\bar{a}$ and $\delta\bar{i}$ are equal to their initial values, and the remaining four differential elements can be propagated using their differential mean rates, which can be obtained from Eqs. (5), to yield the following expressions:

$$\delta\bar{\lambda} = \delta\bar{\lambda}_0 + \delta\dot{\lambda}_s\,\Delta t \tag{28a}$$

$$\delta\bar{q}_1 = \cos(\dot{g}_s\,\Delta t)\;\delta\bar{q}_{10} - \sin(\dot{g}_s\,\Delta t)\;\delta\bar{q}_{20} - \bar{q}_2\delta\dot{g}_s\,\Delta t \tag{28b}$$

$$\delta\bar{q}_2 = \sin(\dot{g}_s\,\Delta t)\;\delta\bar{q}_{10} + \cos(\dot{g}_s\,\Delta t)\;\delta\bar{q}_{20} + \bar{q}_1\delta\dot{g}_s\,\Delta t \tag{28c}$$

$$\delta\bar{h} = \delta\bar{h}_0 + \delta\dot{h}_s\,\Delta t \tag{28d}$$

The differential rates in Eqs. (28) can themselves be rewritten in terms of $\delta\bar{a}$, $\delta\bar{i}$, $\delta\bar{q}_{10}$ and $\delta\bar{q}_{20}$:

$$\begin{aligned}\frac{\delta\dot{\lambda}_s}{\bar{n}} &= \left[-\frac{3}{2} + \frac{21}{8}J\left\{(1+\bar{\eta}) - (5+3\bar{\eta})\cos^2\bar{i}\right\}\right]\frac{\delta\bar{a}}{\bar{a}} - \frac{3}{4}J(5+3\bar{\eta})\sin 2\bar{i}\,\delta\bar{i} \\ &\quad -\frac{3}{4\bar{\eta}^2}J\left[(3+4\bar{\eta}) - (20+9\bar{\eta})\cos^2\bar{i}\right](\bar{q}_{10}\,\delta\bar{q}_{10} + \bar{q}_{20}\,\delta\bar{q}_{20})\end{aligned} \tag{29a}$$

$$\frac{\delta\dot{g}_s}{\bar{n}} = J\left[\frac{21}{8}(1-5\cos^2\bar{i})\frac{\delta\bar{a}}{\bar{a}} - \frac{15}{4}\sin 2\bar{i}\,\delta\bar{i} - \frac{3}{\bar{\eta}^2}(1-5\cos^2\bar{i})\,(\bar{q}_{10}\,\delta\bar{q}_{10} + \bar{q}_{20}\,\delta\bar{q}_{20})\right] \tag{29b}$$

$$\frac{\delta\dot{h}_s}{\bar{n}} = J\left[\frac{21}{4}\cos\bar{i}\,\frac{\delta\bar{a}}{\bar{a}} + \frac{3}{2}\sin\bar{i}\,\delta\bar{i} - \frac{6}{\bar{\eta}^2}\cos\bar{i}\;(\bar{q}_{10}\,\delta\bar{q}_{10} + \bar{q}_{20}\,\delta\bar{q}_{20})\right] \tag{29c}$$

Equations (28) and (29) can be used to formulate the transition matrix for the differential

elements, $\overline{\mathbf{\Phi}}_e(\overline{\boldsymbol{\alpha}}, \Delta t)$, such that $\boldsymbol{\delta}\overline{\boldsymbol{\alpha}}(\Delta t) = \overline{\mathbf{\Phi}}_e(\overline{\boldsymbol{\alpha}}, \Delta t)\, \boldsymbol{\delta}\overline{\boldsymbol{\alpha}}_0$. As a consequence, Eq. (12) can be rewritten as:

$$\widehat{\mathbf{x}}(\Delta t) = [\mathbf{P}_0(\overline{\boldsymbol{\alpha}}) + J\mathbf{P}_J(\overline{\boldsymbol{\alpha}})]\ \overline{\mathbf{\Phi}}_e(\overline{\boldsymbol{\alpha}}, \Delta t)\, \boldsymbol{\delta}\overline{\boldsymbol{\alpha}}_0 \tag{30}$$

The components of $\mathbf{P}_0$ and $\mathbf{P}_J$ are presented in Appendix C.

Averaged Relative Motion near Circular Orbits

Due to oblateness effects, the osculating eccentricity of a satellite's orbit is at least $\mathcal{O}(J_2)$. The average eccentricity, $\widehat{e}$, when $\bar{e} = 0$, cannot be obtained from its short-periodic variation, derived in [20], since using that expression results in $\widehat{e} = 0$. However, the averaged eccentricity for $\bar{e} = 0$ can be obtained from the short-periodic variations of q_1 and q_2 that are derived in [6], by selecting $\bar{q}_1 = \bar{q}_2 = 0$ in the formulae, and then obtaining the average, as shown below:

$$\widehat{e}\,\Big|_{\bar{e}=0} = \frac{1}{2\pi}\int_0^{2\pi} \sqrt{q_{1_{\mathrm{sp}}}^2 + q_{2_{\mathrm{sp}}}^2}\,\Big|_{\bar{q}_1=\bar{q}_2=0}\, d\bar{\lambda} \tag{31}$$

where

$$q_{1_{\mathrm{sp}}}\Big|_{\bar{q}_1=\bar{q}_2=0} = J\left[\frac{7}{8}\sin^2\bar{i}\,\cos 3\bar{\lambda} - \frac{3}{8}(1-5\cos^2\bar{i})\cos\bar{\lambda}\right] \tag{32a}$$

$$q_{2_{\mathrm{sp}}}\Big|_{\bar{q}_1=\bar{q}_2=0} = J\left[\frac{7}{8}\sin^2\bar{i}\,\sin 3\bar{\lambda} - \frac{3}{8}(3-7\cos^2\bar{i})\sin\bar{\lambda}\right] \tag{32b}$$

Although a closed-form solution to Eq. (31) is not known, the integrand is always greater than or equal to zero, and not identically zero, and consequently, $\widehat{e} \neq 0$.

Similarly, the averaged radius, $\widehat{r}$, is not equal to the mean semimajor axis, $\bar{a}$, which would be obtained by simply substituting $\bar{q}_1 = \bar{q}_2 = 0$ and $\bar{\eta} = 1$ in Eq. (16a). The correct value is obtained by assuming $\bar{q}_1 = \bar{q}_2 = 0$ in Eq. (18a), upon which the following is obtained:

$$r\,\Big|_{\bar{q}_1=\bar{q}_2=0} \approx (\bar{r} + r_{\mathrm{sp}})\,\Big|_{\bar{q}_1=\bar{q}_2=0} = \bar{a}\left[1 + \frac{3}{4}J(1-3\cos^2\bar{i}) + \frac{1}{4}J\sin^2\bar{i}\,\cos 2\bar{\lambda}\right] \tag{33}$$

$$\widehat{r}\,\Big|_{\bar{q}_1=\bar{q}_2=0} = \bar{a}\left[1 + \frac{3}{4}J(1-3\cos^2\bar{i})\right] \tag{34}$$

Equation (34) agrees with the simplified expression obtained by Vallado[37], for an orbit with $\bar{e} = 0$.

Upon substituting $\bar{q}_1 = \bar{q}_2 = 0$, $\bar{\eta} = 1$, and $\bar{\theta} = \bar{\lambda}$ in the matrices $\mathbf{P}_0$, $\mathbf{P}_J$, and $\widetilde{\mathbf{\Phi}}_{\bar{e}}$, it can

be shown that the averaged relative position variables are:

$$\begin{aligned}
\widehat{x} &= \left[1-\frac{3}{4}J\left(1-3\cos^2\bar{i}\right)\right]\frac{\delta\bar{a}}{\bar{a}} - \cos(\bar{\lambda}-\dot{g}_s\,\Delta t)\,\delta\bar{q}_{10} - \sin(\bar{\lambda}-\dot{g}_s\,\Delta t)\,\delta\bar{q}_{20} \\
&\quad +\frac{9}{4}J\sin 2\bar{i}\,\delta\bar{i} \qquad (35a)\\
\widehat{y} &= \left[-\frac{3}{2}+\frac{33}{8}J\left(1-3\cos^2\bar{i}\right)\right](\bar{n}\Delta t)\,\frac{\delta\bar{a}}{\bar{a}} + \left[1+\frac{3}{4}J(1-3\cos^2\bar{i})\right]\delta\bar{\lambda}_0 - \frac{21}{4}J\sin 2\bar{i}\,(\bar{n}\Delta t)\,\delta\bar{i} \\
&\quad +2\sin(\bar{\lambda}-\dot{g}_s\Delta t)\,\delta\bar{q}_{10} - 2\cos(\lambda-\dot{g}_s\Delta t)\,\delta\bar{q}_{20} + \left[1+\frac{3}{4}J\left(1-3\cos^2\bar{i}\right)\right]\cos\bar{i}\,\delta\bar{h}_0 \qquad (35b)\\
\widehat{z} &= -\frac{21}{8}J\sin 2\bar{i}\,\cos\bar{\lambda}\,(\bar{n}\Delta t)\,\frac{\delta\bar{a}}{\bar{a}} + \left[\sin\bar{\lambda}-\frac{3}{2}J\sin^2\bar{i}\,\cos\bar{\lambda}\,(\bar{n}\Delta t)\right]\delta\bar{i} - \cos\bar{\lambda}\,\sin\bar{i}\,\delta\bar{h}_0 \\
&\quad -\frac{3}{4}J\sin 2\bar{i}\,\delta\bar{q}_{10} - \frac{3}{4}J\sin 2\bar{i}\,\delta\bar{q}_{20} \qquad (35c)
\end{aligned}$$

In an unperturbed gravitation field, under the assumption of small orbital element differences, out-of-plane displacement depends only upon the differential inclination and right ascension, and is consequently decoupled from in-plane motion. It is easily seen that the J_2 perturbation introduces coupling. Furthermore, the out-of-plane frequency is $\dot{\lambda}_s = \dot{g}_s + \dot{l}_s$, is seen to be different from the in-plane frequency, which is given by $\dot{\lambda}_s - \dot{g}_s = \dot{l}_s$. It is also observed from Eq. (35c) that the J_2 perturbation causes secular growth in the out-of-plane direction. What is perhaps more interesting, is the appearance of bias terms in the radial position. This bias exists even when the two-body condition for zero radial bias, $\delta\bar{a} = 0$, is satisfied. For relative motion near an elliptic orbit, additional bias terms of $\mathcal{O}(J_2)$, that are dependent on δi, δq_1, and δq_2, also exist, as can be seen from the first row of the matrix $\mathbf{P}_J$ in Appendix C. These effects are studied in detail in the next section.

Effects of J_2 on Bounded Relative Motion

From Eq. (35b), it is observed that even if $\delta\bar{a} = 0$, which ensures bounded relative motion in the two body problem, several terms of $\mathcal{O}(J_2)$ contribute to secular growth. An along-track correction assuming small differential orbital elements, correct to the first order in J_2, and for low eccentricities, was derived by Vadali *et al.*[38]. Their work used a mean element formulation, and canceled secular growth terms by using the so-called "rate-matching" condition, given by:

$$\delta\dot{g}_s + \delta\dot{l}_s + \delta\dot{h}_s\,\cos\bar{i} = 0 \qquad (36)$$

Upon examining the more general expression for averaged along-track motion that is valid for non-circular orbits, it can be shown that the terms contributing to secular growth are

given by

$$\left[P_{0_{22}}\delta\dot{\lambda}_s - (\bar{q}_2 P_{0_{24}} - \bar{q}_1 P_{0_{25}})\,\delta\dot{g}_s + P_{0_{26}}\delta\dot{h}_s\right]\,\Delta t \tag{37}$$

The corresponding terms from the matrix $J\mathbf{P}_J$ are ignored because their contribution is only to $\mathcal{O}(J_2^2)$, and because $\delta\bar{a} = \mathcal{O}(J_2)$ for bounded relative motion. Equation (37) is completely expressed in terms of mean elements and mean differential elements, if Eqs. (29) are used. However, since $\mathbf{P}_0$ is generally time-varying, Eq. (37) cannot be identically zero. Therefore, the rate-matching constraint of [38] is used to bound along-track motion (out-of-plane motion is still unbounded due to J_2). Substituting Eqs. (29) in Eq. (36) results in the following expression for $\delta\bar{a}$[32]:

$$\frac{\delta\bar{a}}{\bar{a}} = -\frac{1}{2}J(4+3\bar{\eta})\left[\sin 2\bar{i}\,\delta\bar{i} + \frac{1}{\bar{\eta}^2}(1-3\cos^2\bar{i})(\bar{q}_{10}\,\delta\bar{q}_{10} + \bar{q}_{20}\,\delta\bar{q}_{20})\right] \tag{38}$$

From the first row of $\mathbf{P}_J$ in Appendix C, it is observed that non-zero values of $\delta\bar{i}$, $\delta\bar{q}_{10}$ and $\delta\bar{q}_{20}$ result in a bias of $\mathcal{O}(J_2)$ in the radial direction. The use of mean elements in the transformation matrix in [6] does not yield this result. Furthermore, if Eq. (38) is made use of, then additional bias terms of $\mathcal{O}(J_2)$ are introduced in the radial direction through $\delta\bar{a}$. The resultant bias is given by:

$$\widehat{x}_{\text{bias}} \;\approx\; \left(\frac{1}{2\pi}\int_0^{2\pi} P_{0_{11}}\,d\bar{l}\right)\frac{\delta\bar{a}}{\bar{a}} + J\left(P_{J_{13}}\,\delta\bar{i} + P_{J_{14}}\,\delta\bar{q}_{10} + P_{J_{15}}\,\delta\bar{q}_{20}\right) \tag{39}$$

Using results from Appendix A, the integral coefficient of $\delta\bar{a}/\bar{a}$ in Eq. (39) can be shown to have a value of $\bar{\eta}^2$. For circular reference orbits, $\bar{x}_{\text{bias}} = -(5/4)J\sin 2\bar{i}\,\delta\bar{i}$. A similar (although small) bias exists in the along-track velocity, due to non-zero semimajor axis difference. This bias, may be calculated in a manner similar to $\bar{x}_{\text{bias}}$, but by using $P_{0_{51}}$, and $P_{J_{53\ldots55}}$. It can also be shown that $(1/2\pi)\int_0^{2\pi} P_{0_{51}}\,d\bar{l} = -3\bar{\eta}/2$.

Design of a Filter for Short-Periodic Perturbations

In this section, the use of averaged relative motion equations is made for the design of filters that remove short-periodic variations in relative states, due to first-order J_2 perturbations. The osculating differential orbital elements corresponding to the relative states, assuming small magnitudes of relative position and velocity, can be obtained as follows:

$$\{\delta a\ \delta\theta\ \delta i\ \delta q_1\ \delta q_2\ \delta\Omega\}^\top = \mathbf{\Sigma}^{-1}(\boldsymbol{\alpha})\,\mathbf{\Gamma}(\overline{\boldsymbol{\alpha}})\,\mathbf{x} \tag{40}$$

where $\boldsymbol{\Sigma}(\boldsymbol{\alpha e})$ is the transformation matrix for osculating elements provided by [6], and $\boldsymbol{\Gamma}(\overline{\boldsymbol{\alpha e}})$ is the 6×6 permutation and scaling matrix that transforms from unscaled to scaled states, whose non-zero entries are given by:

$$\Gamma_{11} = \Gamma_{32} = \Gamma_{53} = \bar{a}, \quad \Gamma_{24} = \Gamma_{45} = \Gamma_{66} = \bar{n}\bar{a} \tag{41}$$

The inverse of this matrix, $\boldsymbol{\Gamma}^{-1}$ can easily be obtained by inspection.

The differential mean elements can be obtained from the differential osculating elements, using the inverse of the matrix $\mathbf{D}(\overline{\boldsymbol{\alpha e}})$ derived in [6], or by the vector $\mathbf{D}(\overline{\boldsymbol{\alpha e}})\,\boldsymbol{\Sigma}^{-1}(\boldsymbol{\alpha e})\,\boldsymbol{\Gamma}(\overline{\boldsymbol{\alpha e}})\,\mathbf{x}$ Furthermore, the differential mean semimajor axis $\delta\bar{a}$ is scaled by the mean semimajor axis $\bar{a}$, and $\delta\bar{\theta}$ is written in terms of the elements $\delta\bar{\lambda}$, $\delta\bar{q}_1$, and $\delta\bar{q}_2$ to yield the vector $\boldsymbol{\delta}\overline{\boldsymbol{\alpha e}}$. Consequently, $\boldsymbol{\delta}\overline{\boldsymbol{\alpha e}} = \mathbf{P}_e(\overline{\boldsymbol{\alpha e}})\,\mathbf{D}(\overline{\boldsymbol{\alpha e}})\,\boldsymbol{\Sigma}^{-1}(\boldsymbol{\alpha e})\,\boldsymbol{\Gamma}(\overline{\boldsymbol{\alpha e}})\,\mathbf{x}$ where the non-zero entries of $\mathbf{P}_e(\overline{\boldsymbol{\alpha e}})$ are given by

$$P_{e_{11}} = 1/\bar{a},\ P_{e_{22}} = 1/\bar{\gamma}_1,\ P_{e_{24}} = -\bar{\gamma}_2/\bar{\gamma}_1, \quad P_{e_{25}} = -\bar{\gamma}_3/\bar{\gamma}_1,\ P_{e_{33}} = P_{e_{44}} = P_{e_{55}} = P_{e_{66}} = 1 \tag{42}$$

The inverse of $\mathbf{P}_e(\overline{\boldsymbol{\alpha e}})$ is also easily obtained by inspection.

The above derivation results in the following:

$$\widehat{\mathbf{x}} \;=\; \underbrace{\left[\mathbf{P}_0(\overline{\boldsymbol{\alpha e}}) + J\mathbf{P}_J(\overline{\boldsymbol{\alpha e}})\right]\,\mathbf{P}_e(\overline{\boldsymbol{\alpha e}})\,\mathbf{D}^{-1}(\overline{\boldsymbol{\alpha e}})\,\boldsymbol{\Sigma}^{-1}(\boldsymbol{\alpha e})\,\boldsymbol{\Gamma}(\overline{\boldsymbol{\alpha e}})}_{\mathbf{F}}\,\mathbf{x} \tag{43}$$

where $\mathbf{F}$ is the filter matrix for short-periodic variations. This paper assumes that the current osculating orbital elements of the chief, and relative position and velocity between the satellites, are known accurately. The mean nonsingular elements of the chief can be obtained from the osculating nonsingular elements, from the first-order correction derived in [6], by simply using $-J_2$ instead of J_2 in the conversion from mean to osculating elements. Similarly, since $\mathbf{D} = [\mathbb{1}_6 + \mathcal{O}(J_2)]$, the inverse of $\mathbf{D}(\overline{\boldsymbol{\alpha e}})$ can also be obtained by using $-J_2$ instead of J_2 in the computation of $\mathbf{D}(\overline{\boldsymbol{\alpha e}})$. Consequently, the matrix $\mathbf{F}$ is completely determined in terms of the chief's mean orbital elements. Furthermore, no matrix inversion operations are necessary since the elements of the matrix $\boldsymbol{\Sigma}^{-1}$ are given in [6].

It may be noted here that a development similar to what is shown above, can be used to derive a "mean filter". In this case, the mean relative states $\overline{\mathbf{x}}$ are obtained by using the transformation matrix for mean elements, $\overline{\boldsymbol{\Sigma}}$, to yield the mean filter matrix $\widetilde{\mathbf{F}}$:

$$\overline{\mathbf{x}} = \widetilde{\mathbf{F}}\,\mathbf{x} \tag{44a}$$

$$\text{where,} \qquad \widetilde{\mathbf{F}} = \boldsymbol{\Gamma}^{-1}(\overline{\boldsymbol{\alpha e}})\,\overline{\boldsymbol{\Sigma}}(\overline{\boldsymbol{\alpha e}})\,\mathbf{D}^{-1}(\overline{\boldsymbol{\alpha e}})\,\boldsymbol{\Sigma}^{-1}(\boldsymbol{\alpha e})\,\boldsymbol{\Gamma}(\overline{\boldsymbol{\alpha e}}) \tag{44b}$$

Formation-Keeping with Disturbance Accommodation

In this section, the application of the analytical filter, to formation-keeping using continuous control, is analyzed. The purpose is to design a control law that does not respond to short-periodic perturbations due to J_2. A linear quadratic regulator (LQR), based on the linearized rendezvous equations for the two-body problem is used. This system is given by the following equations:

$$\ddot{\xi} - 2\dot{\theta}\dot{\vartheta} - \left(\dot{\theta}^2 + 2\frac{\mu}{r^3}\right)\xi - \ddot{\theta}\vartheta = u_\xi \tag{45a}$$

$$\ddot{\vartheta} + 2\dot{\theta}\dot{\xi} - \left(\dot{\theta}^2 - \frac{\mu}{r^3}\right)\vartheta + \ddot{\theta}\xi = u_\vartheta \tag{45b}$$

$$\ddot{\zeta} + \frac{\mu}{r^3}\zeta = u_\zeta \tag{45c}$$

where the coefficients of the states are functions of the orbital elements of the chief satellite. The position variables are scaled by $\bar{a}$, and the velocity variables by $\bar{n}\bar{a}$, which are identical to a and na, respectively, in a central gravity field. Furthermore, Eqs. (16a) and (16d) are used to rewrite the linear system for rendezvous in the following form:

$$\mathbf{x}' = \mathbf{A}\mathbf{x} + \mathbf{B}\hat{\mathbf{u}} \tag{46}$$

where,

$$\hat{\mathbf{u}} = 1/(\bar{n}^2\bar{a})\left\{u_\xi \; u_\vartheta \; u_\zeta\right\}^\top, \quad \mathbf{B} = \left[\mathbb{O}_3 \; \mathbb{1}_3\right]^\top \tag{47a}$$

$$\mathbf{A} = \begin{bmatrix} \mathbb{O}_3 & \mathbb{1}_3 \\ \widetilde{\mathbf{A}} & \boldsymbol{\Omega} \end{bmatrix}, \; \widetilde{\mathbf{A}} = \frac{\bar{\alpha}^3}{\bar{\eta}^6}\begin{bmatrix} (\bar{\alpha}+2) & -2\bar{\beta} & 0 \\ 2\bar{\beta} & (\bar{\alpha}-1) & 0 \\ 0 & 0 & -1 \end{bmatrix}, \; \boldsymbol{\Omega} = \frac{2\bar{\alpha}^2}{\bar{\eta}^3}\begin{bmatrix} 0 & 1 & 0 \\ -1 & 0 & 0 \\ 0 & 0 & 0 \end{bmatrix} \tag{47b}$$

The matrices $\mathbf{A}$ and $\mathbf{B}$ are periodic, but implicit in time. Furthermore, mean elements are used throughout to evaluate the matrices.

As shown in [39], periodic solutions to this system are given by:

$$x_\wp = \rho_1 \sin(\bar{\theta} + \phi_0) \tag{48a}$$

$$y_\wp = \rho_1 \cos(\bar{\theta} + \phi_0)\frac{(\bar{\alpha}+1)}{\bar{\alpha}} + \frac{\rho_2}{\bar{\alpha}} \tag{48b}$$

$$z_\wp = \rho_3 \frac{\sin(\bar{\theta} + \psi_0)}{\bar{\alpha}} \tag{48c}$$

where $\rho_{1,2,3}$, ϕ_0, and ψ_0 are constant design parameters. The relative velocities can easily be

derived and are as follows:

$$x'_{\wp} = \frac{\rho_1}{\bar{\eta}^3}\cos(\bar{\theta}+\phi_0)\,\bar{\alpha}^2 \tag{49a}$$

$$y'_{\wp} = -\frac{\rho_1}{\bar{\eta}^3}\left[\sin(\bar{\theta}+\phi_0)\,\bar{\alpha}(\bar{\alpha}+1) - \cos(\bar{\theta}+\phi_0)\,\bar{\beta}\right] + \frac{\rho_2}{\bar{\eta}^3}\bar{\beta} \tag{49b}$$

$$z'_{\wp} = \frac{\rho_3}{\bar{\eta}^3}\left[\cos(\bar{\theta}+\psi_0)\,\bar{\alpha} + \sin(\bar{\theta}+\psi_0)\,\bar{\beta}\right] \tag{49c}$$

These solutions are valid for all values of eccentricity, although implicit in time, and for small relative distances, in the absence of perturbations.

A control based on LQR design is desired, for the following system and cost function:

$$\boldsymbol{\Delta}\mathbf{x}' = \mathbf{A}\,\boldsymbol{\Delta}\mathbf{x} + \mathbf{B}\hat{\mathbf{u}} + \mathbf{d} \tag{50a}$$

$$\mathcal{J} = \frac{1}{2}\int_0^\infty \left(\boldsymbol{\Delta}\mathbf{x}^\top\mathbf{Q}\boldsymbol{\Delta}\mathbf{x} + \hat{\mathbf{u}}^\top\mathbf{R}\hat{\mathbf{u}}\right)\,d\tau \tag{50b}$$

where $\tau = \bar{n}\,t$, $\boldsymbol{\Delta}\mathbf{x} = \mathbf{x} - \mathbf{x}_{\text{ref}}$ is the error between the current states $\mathbf{x}$ and the reference states $\mathbf{x}_{\text{ref}}$, and $\mathbf{d}$ is the vector of unmodeled disturbances. The matrices $\mathbf{Q}$ and $\mathbf{R}$ are weight matrices that indicate the relative importance of the fuel cost and deviation from the reference trajectory.

The reference trajectory is not necessarily a natural solution of the system, and in this section, the choice $\mathbf{x}_{\text{ref}} = \mathbf{x}_{\wp}$ is made, where the individual reference states are given by Eqs. (48) and Eqs. (49). The unmodeled disturbance vector is composed of nonlinearities in the differential gravity, and J_2 perturbations. It is worth noting that reference trajectories that account for higher-order nonlinearity effects[40–42] may also be used; however, since the focus of this section is on the application of the filter for short-periodic perturbations, their use was not explored as they further complicate analysis. Furthermore, for small relative orbits, J_2-induced effects dominate over nonlinearity effects[10].

Control effort is always required to counter the effects of $\mathbf{d}$. Ideally, the controls should not respond to short-periodic variations in the relative states, and for this reason, several bias and frequency filters, by the introduction of additional states, were used in the formation-keeping problem for perturbed, circular orbits, in [12]. Instead of adding additional states that require numerical integration, the analytical filter given by Eq. (43) can be used effectively. The details of the derivation of the feedback law are available in [43], and are not presented here. It is sufficient to note here that the control effort is given by $\hat{\mathbf{u}} = -\mathbf{K}\,\boldsymbol{\Delta}\mathbf{x}$, where $\mathbf{K}$ is the gain matrix obtained by solving the Riccati equation[43] by numerical integration, over one orbit of the chief. Since the linearized system of equations is 2π-periodic, these gains can be used over successive orbits. Instead of feeding back the actual osculating states $\mathbf{x}$, the average

states $\widehat{\mathbf{x}}$, obtained from Eq. (43), are used. Consequently, $\hat{\mathbf{u}} = -\mathbf{K}\left(\widehat{\mathbf{x}} - \mathbf{x}_{\wp}\right) = -\mathbf{K}\left(\mathbf{F}\mathbf{x} - \mathbf{x}_{\wp}\right)$.

Numerical Examples

In this section, numerical examples are used to demonstrate the use of averaged relative motion equations. The first example compares the results of the mean, osculating, and averaged formulations of relative motion. The second demonstrates the use of the short-periodic filter, given by Eq. (43), for formation-keeping near an elliptic orbit. Furthermore, the effects of tracking a modified reference trajectory that accounts for bias in the radial direction, is studied.

Mean, Osculating, and Averaged Relative Motion

An example from [6] is considered, to test the results of this paper. Consider a reference orbit with the following initial mean orbital elements:

$$\begin{aligned} \bar{a} = 7,091.870\,\text{km}, \quad \bar{\theta}_0 = 3.141596\,\text{rad}, \quad \bar{i} = 1.221521\,\text{rad} \\ \bar{q}_{10} = 0.00523, \qquad \bar{q}_{20} = 0.001709, \qquad \bar{h}_0 = 0.7853999\,\text{rad} \end{aligned} \tag{51}$$

Relative motion is established by selecting the following initial mean differential orbital elements

$$\begin{aligned} \delta\bar{a} = 0.415\,\text{m} \qquad \delta\bar{\lambda}_0 = -6.195769 \times 10^{-7}\,\text{rad} \quad \delta\bar{i} = -7.079055 \times 10^{-5}\,\text{rad} \\ \delta\bar{q}_{10} = 1.601 \times 10^{-7} \qquad \delta\bar{q}_{20} = 3.561 \times 10^{-5} \qquad \delta\bar{h}_0 = 0\,\text{rad} \end{aligned} \tag{52}$$

The mean elements of the deputy and chief are converted to osculating elements using Brouwer theory, and then converted to ECI position and velocity. These are used as initial conditions to numerically integrate the equations of motion in the ECI frame, for each satellite. The true relative position and velocity are then obtained by transforming the inertial position and velocity differences into the LVLH frame of the chief.

For comparison, three errors are defined:

1. Osculating error, or the error between the states as predicted by the Gim-Alfriend transformation matrix for osculating elements, $\boldsymbol{\Sigma}$, and the relative states obtained from numerical integration of the ECI equations.

2. Mean error, or the error between the states obtained by using a linearized transformation between differential elements and states, that uses mean elements. For example, the mean transformation matrix $\overline{\boldsymbol{\Sigma}}$, derived in [6].

3. Average error, that is obtained by adding the correction matrix $J\mathbf{P}_J$ to the relative states obtained using P_0.

The three errors are shown for the radial, along-track and out-of-plane directions, in Figs. 1, 2, and 3, respectively. In these figures, the solid curve indicates the osculating error over 10 orbits, and these are identical to the results shown in [6]. The dotted curve indicates the mean error, and the dashed curve indicates the error after correction. It is observed that the radial correction to the position, depicted by Fig. 1(a), is the most beneficial among the three position errors, and this is a consequence of the short-periodic correction to the satellite radius, presented in this paper. Although the along-track error, Fig. 2(a) shows secular growth and out-of-plane error, Fig. 3(a), shows a non-zero bias, the mean values of the respective errors upon using the correction are the same as that using osculating elements. The growth and bias are consequences of linearization; if higher-order terms in the map from differential orbital elements, to relative states is used, as shown in [32], these effects can be removed, although the use of nonlinear terms was not explored. These figures also show the usefulness of the matrices $\mathbf{P}_0$ and $\mathbf{P}_J$, for the purpose of tracking an averaged orbit. If a tracking controller design is desired such that short-periodic perturbations due to J_2 (or any perturbation that can be obtained via a generating function) are ignored, then in effect, what is desired is a tracking profile indicated by the dashed curves in Figs. 1, 2, and 3. The mean error as shown by this indicator, is essentially the difference between the actual state that contains short- and long-periodic variations, and the average state as obtained by the matrices $\mathbf{P}_0$ and $\mathbf{P}_J$.

The velocity errors are shown in Fig. 1(b), Fig. 2(b), and Fig. 3(b). There is no improvement in the radial velocity, as shown by Fig. 1(b); in fact the bias correction is found to be zero. It can also be shown that the average short-periodic variation in radial velocity is zero. The bias due to the use of mean elements, as well as the improvement in the out-of-plane velocity, Fig. 3(b), are observed to be negligible for low eccentricities, although the effect of the correction is more pronounced for higher eccentricities. As shown in Fig. 2(b), the along-track velocity correction is the most significant among the three.

Formation-Keeping Using the Short-Periodic Variation Filter

A reference orbit with the following mean initial orbital elements is considered:

$$\begin{aligned} \bar{a} = 7,191.870\,\text{km}, \quad \bar{\theta}_0 = 3.141596\,\text{rad}, \quad \bar{i} = 1.221521\,\text{rad} \\ \bar{q}_{10} = 0.0523, \qquad \bar{q}_{20} = 0.01709, \qquad \bar{h}_0 = 0.7853999\,\text{rad} \end{aligned} \tag{53}$$

This reference orbit has a mean eccentricity of 0.055, which is 10 times the eccentricity of the reference orbit chosen in the previous example. Consequently, a slightly higher value is chosen for the mean semimajor axis, to ensure the perigee of the orbit does not approach too close to the planetary surface. Based on the relative orbit parameterization given by

Eq. (48), the following are chosen as parameters for the mean relative orbit for tracking:

$$\rho_1 = 250\,\mathrm{m}, \quad \rho_2 = -7.5\,\mathrm{m}, \quad \rho_3 = 500\,\mathrm{m}, \quad \phi_0 = \psi_0 = 0 \tag{54}$$

These parameters correspond to a relative orbit that projects to an approximate circle in the θ-h plane, of radius 500 m. The phase parameters ϕ_0 and ψ_0 indicate that the relative orbit was established using an inclination difference between the deputy and chief orbit's, and without a right ascension difference[39]. It is well-known that such relative orbits require more fuel for formation-keeping than those established using a right ascension difference only.

In this example, the weight matrices on the states and control are selected as $\mathbf{Q} = \mathbb{1}_6$, and $\mathbf{R} = \mathbb{1}_3$, respectively. The control effort used for formation-keeping, for ten orbits of the chief, using the unfiltered (osculating) states as feedback, is shown in Fig. 4, and is depicted by the solid curve. It is observed that the radial control oscillates about a non-zero bias. The tracking of a periodic orbit with parameters specified by Eq. (54) implicitly assumes that along-track rates are matched, although the non-zero inclination difference will result in out-of-plane growth. As a consequence, the differential semimajor axis is non-zero, and this contributes the term $\overline{x}_{\text{bias}}$ to the radial position, as shown in Eq. (39). Therefore, also of interest is the result of tracking a new reference orbit, whose radial position includes the bias, i.e., $x_\wp + \overline{x}_{\text{bias}}$ is the new reference radial position. As a result of using this new reference solution, the desired relative orbit is slightly offset in the radial direction. The result of tracking this new orbit is depicted by the dotted curve in Fig. 4. It is observed that the bias in the radial control is removed; however, the control effort in the along-track and out-of-plane are not noticeably changed, as is observed from the solid and dotted curves. The dashed curve depicts the control effort if the averaging filter $\mathbf{F}$ is applied to the measured states $\mathbf{x}$ prior to feeding them back into the control law. An improvement is immediately observed in the radial and along-track controls, since the control effort in these axes are free from short-periodic oscillations and are approximately equal to the mean value of control using unfiltered states. Although a significant improvement is not observed in the out-of-plane control, the short-periodic variations are still absent in the control with filtered states. The high amplitude of the control is required to track bounded motion in the out-of-plane direction.

Figure 5, shows the resulting position error LQR-based formation-keeping. The position error using unfiltered states is on an average, 1 m (solid curve), which is approximately 0.2% of the orbit size. This error can be decreased or increased by changing the value of the weight matrix $\mathbf{Q}$. The use of a bias-corrected reference trajectory (dotted curve) reduces the

error to an average of 0.5 m. The use of the short-periodic filter (dashed curve) increases the amplitude of the error; however, the average of this error is the same as that achieved by tracking the bias-corrected trajectory (dashed curve).

The cost required for formation-keeping is shown in Fig. 6. The cost is calculated as the result of the integral $\frac{1}{2}\int_0^{\tau_f}(\hat{u}_r^2+\hat{u}_\theta^2+\hat{u}_h^2)\,d\tau$ where $\tau_f = 10\cdot 2\pi$, which is the normalized time for ten orbits of the chief. By using the new reference solution, the cost for formation-keeping is reduced by 50%, as can be observed by comparing the solid and dotted curves. The use of filtered feedback (dashed curve) further reduces the cost to approximately 20% of the cost of unfiltered feedback without bias correction or to 30% of the cost of unfiltered feedback with bias correction.

The dashed-dotted curves in Figs. 4, 5, and 6 are the result of using the mean filter $\widetilde{\mathbf{F}}$, given by Eq. (44), instead of the averaging filter. Although the radial control using the mean filter shows low response to the short-periodic variations in the states, the average value of this control differs from those corresponding to the unfiltered control or control using $\mathbf{F}$ (dotted and dashed curves, respectively). This results in the relative trajectory approaching a relative orbit that is different from the desired. As shown in Fig. 5, the corresponding position error is 2 m, which is larger than the error using unfiltered state feedback. Furthermore, the cost associated with the filter $\widetilde{\mathbf{F}}$ is higher than that obtained using the averaging filter, as shown in Fig. 6. In some cases, it was observed that the cost using $\widetilde{\mathbf{F}}$ could possibly be lower than using the averaged filter. This was a consequence of the average value of the control using $\widetilde{\mathbf{F}}$ being lower than that obtained using $\mathbf{F}$. It is important to note, however, that this control is essentially incorrect, and results in larger state errors with a larger bias than those obtained using unfiltered states.

In this section it is shown that the use of the averaging filter can significantly reduce costs by removing short-periodic variations in the relative states. The number of computations required is not significantly larger than that used for mean elements, since the matrix $\mathbf{P}_J$ depends only on the mean semimajor axis, eccentricity, and inclination of the chief satellite, and has to be evaluated only once. Furthermore, it is also shown that using reference solutions that account for J_2 effects will further reduce fuel required for stationkeeping.

Conclusions

The work in this paper has successfully developed averaged expressions for relative motion. The number of computations required to calculate the average states are far lower than those required to calculate the osculating states. For small relative orbits, the errors between osculating and averaged states, are of the order of centimeters, although the errors between osculating and mean states are more significant. Furthermore, as the orbit size increases,

the bias in error introduced by the use of mean elements also increases, and the use of the correction matrix $\mathbf{P}_J$ becomes more important. However, the bias due to linearization also increases, so it may be necessary to introduce second-order terms. The advantage, as shown in [11], is that the higher-order terms can be introduced using mean elements only, thereby resulting in a complete, mean-element description of relative motion. The use of higher-order tensors was not explored in this paper.

The use of averaged relative states also provides additional insight into the effects of J_2 on relative orbits. In particular, some combinations of initial conditions are shown to result in a bias in the radial direction. Consequently, tracking a reference solution that does not account for this bias is shown to result in higher fuel cost. The matrices $\mathbf{P}_0$ and $\mathbf{P}_J$ can also be used as an analytical filter to remove J_2-induced short-periodic perturbations from the osculating (actual) states, if the elements of the chief are known. The use of this analytical filter has been demonstrated in the design of feedback laws for formation-keeping, and helps avoid the use of numerical filtering techniques for disturbance accommodation.

Appendix A: Solution to I_{mk}

The key step in solving integrals of type shown in Eq. (19a), is the complex change of variable, $\exp(\jmath f) = \chi$. Also used are the expressions $dl = \eta^3\, df/(1+e\cos f)^2$, and $(1+e\cos f) = e\,(\chi+\varepsilon)(\chi+1/\varepsilon)/(2\chi)$. After some algebra, it can be shown that:

$$I_{mk} = -\frac{\jmath\eta^3}{2\pi}\left(\frac{2}{e}\right)^{m+2}\oint \frac{\chi^{k+m+1}}{(\chi+\varepsilon)^{m+2}(\chi+1/\varepsilon)^{m+2}}\,d\chi \tag{A1}$$

For $m+2>0$, the terms in the denominator of the integrand in Eq. (A1) can be split into partial fractions as shown below:

$$\begin{aligned}\frac{1}{(\chi+\varepsilon)^{m+2}\,(\chi+1/\varepsilon)^{m+2}} \;=\; &\left(\frac{e}{2\eta}\right)^{m+2}\frac{1}{(m+1)!}\sum_{j=1}^{m+2}\left\{\left(-\frac{e}{2\eta}\right)^{j-1}\frac{(m+j)!}{(j-1)!}\right.\\ &\left.\times\left[\frac{1}{(\chi+\varepsilon)^{m-j+3}}+\frac{(-1)^{m-j+3}}{(\chi+1/\varepsilon)^{m-j+3}}\right]\right\}\end{aligned} \tag{A2}$$

By using the fact that $|\varepsilon|<1$ and $|1/\varepsilon|>1$, and from Cauchy's integral formula, the following can be established:

$$\oint \frac{\chi^{k+m+1}\,d\chi}{(\chi+1/\varepsilon)^{m-j+3}} = 0, \quad \oint \frac{\chi^{k+m+1}\,d\chi}{(\chi+\varepsilon)^{m-j+3}} = 2\pi\jmath\frac{(k+m+1)!}{(m-j+2)!\,(k+j-1)!}\,(-\varepsilon)^{j+k-1} \tag{A3}$$

Upon substituting Eq. (A2) and Eq. (A3) in Eq. (A1), the integral I_{mk} can be solved, to yield the following result:

$$I_{mk} = \frac{(-\varepsilon)^k}{\eta^{m-1}} \frac{(k+m+1)!}{(m+1)!} \sum_{j=0}^{m+1} \frac{(m+j+1)!}{j!\,(m-j+1)!\,(k+j)!} \left(\frac{e\varepsilon}{2\eta}\right)^j \tag{A4}$$

Appendix B: Solution to I_0

In this appendix, a series solution to Eq. (19b) is found. In [16], an expression for $f - l$, which is known as the equation of the center, is provided in terms of Bessel functions, and harmonics of the mean anomaly. However, to calculate definite integrals with specified limits of integration, it is easier to use a series in the eccentric anomaly, which has coefficients that are not themselves series in a small parameter. From Eq. (1), it can be shown that:

$$\frac{df}{dE} = \frac{\eta}{1 - e\cos E} \tag{B1}$$

Using a Fourier series as shown by Battin[16] and Sengupta and Vadali[39], the following expressions can be developed:

$$\frac{1}{(1+e\cos f)} = \frac{1}{\eta} + \frac{2}{\eta}\sum_{p=1}^{\infty}(-\varepsilon)^p \cos pf \tag{B2a}$$

$$\frac{1}{(1-e\cos E)} = \frac{1}{\eta} + \frac{2}{\eta}\sum_{p=1}^{\infty}\varepsilon^p \cos pE \tag{B2b}$$

where ε was defined in Eq. (21), and $p \in \mathbb{Z}_{>0}$. It follows that Eq. (B1) may be rewritten as:

$$df = \left[1 + 2\sum_{p=1}^{\infty}\varepsilon^p \cos pE\right] dE \tag{B3}$$

and consequently,

$$f = E + 2\sum_{p=1}^{\infty}\frac{\varepsilon^p}{p}\sin pE \tag{B4}$$

Finally, from Kepler's equation,

$$l = E - e\sin E \Rightarrow dl = (1 - e\cos E)\,dE \tag{B5}$$

Upon substituting Eq. (B4) and Eq. (B5) in Eq. (19b), it can be shown that when $\varrho(f) = 1/(1+e\cos f)^m$, the following is true:

$$I_0 = \frac{1}{\eta^{2m}} \int_0^{2\pi} \left[e\sin E - \frac{e^2}{2}\sin 2E + \sum_{p=1}^{\infty} \frac{\varepsilon^p}{p} \left(2\sin pE - e\sin\overline{p+1}E - e\sin\overline{p-1}E \right) \right] \times (1-e\cos E)^m \, dE \tag{B6}$$

Equation (B6) can be integrated easily if m is known. Since the integrand is an odd function, $I_0 = 0 \ \forall m$. This is also true when $\varrho(f) = \cos f/(1+e\cos f)^m$. However, when $\varrho(f) = \sin f/(1+e\cos f)^m$, the integrand has some components that are even functions. In particular, it is easy to show using Eq. (B6), that:

$$\frac{1}{2\pi}\int_0^{2\pi} (f-l)\sin f \, dl = \frac{\varepsilon\eta}{2}\frac{(3+\eta)}{(2+\eta)} \tag{B7a}$$

$$\frac{1}{2\pi}\int_0^{2\pi} \frac{(f-l)\sin f \, dl}{(1+e\cos f)} = \frac{\varepsilon}{4\eta}(5+3\eta) \tag{B7b}$$

Appendix C: Matrices $\mathbf{P}_0$ and $\mathbf{P}_J$

The components of $\mathbf{P}_0$ and $\mathbf{P}_J$ are as follows:

$$P_{011} = \frac{\bar{\eta}^2}{\bar{\alpha}} \tag{C1a}$$

$$P_{012} = \frac{\bar{\beta}}{\bar{\eta}} \tag{C1b}$$

$$P_{013} = 0 \tag{C1c}$$

$$P_{014} = \frac{\bar{q}_1\bar{q}_2\sin\bar{\theta}}{\bar{\eta}(1+\bar{\eta})} - \frac{(1+\bar{\eta}-\bar{q}_1{}^2)\cos\bar{\theta}}{\bar{\eta}(1+\bar{\eta})} \tag{C1d}$$

$$P_{015} = \frac{\bar{q}_1\bar{q}_2\cos\bar{\theta}}{\bar{\eta}(1+\bar{\eta})} - \frac{(1+\bar{\eta}-\bar{q}_2{}^2)\sin\bar{\theta}}{\bar{\eta}(1+\bar{\eta})} \tag{C1e}$$

$$P_{016} = 0 \tag{C1f}$$

$$P_{021} = 0 \tag{C2a}$$

$$P_{022} = \frac{\bar{\alpha}}{\bar{\eta}} \tag{C2b}$$

$$P_{023} = 0 \tag{C2c}$$

$$P_{024} = \frac{\bar{q}_2\bar{\alpha}}{(1+\bar{\eta})\bar{\eta}} + \sin\bar{\theta} + \frac{\bar{q}_2+\sin\bar{\theta}}{\bar{\alpha}} \tag{C2d}$$

$$P_{025} = -\frac{\bar{q}_1\bar{\alpha}}{(1+\bar{\eta})\bar{\eta}} - \cos\bar{\theta} - \frac{\bar{q}_1 + \cos\bar{\theta}}{\bar{\alpha}} \tag{C2e}$$

$$P_{026} = \frac{\bar{\eta}^2}{\bar{\alpha}}\cos\bar{i} \tag{C2f}$$

$$P_{031} = 0 \tag{C3a}$$

$$P_{032} = 0 \tag{C3b}$$

$$P_{033} = \frac{\bar{\eta}^2}{\bar{\alpha}}\sin\bar{\theta} \tag{C3c}$$

$$P_{034} = 0 \tag{C3d}$$

$$P_{035} = 0 \tag{C3e}$$

$$P_{036} = -\frac{\bar{\eta}^2}{\bar{\alpha}}\cos\bar{\theta}\,\sin\bar{i} \tag{C3f}$$

$$P_{041} = -\frac{\bar{\beta}}{2\eta} \tag{C4a}$$

$$P_{042} = -\frac{\bar{\alpha}^2}{\bar{\eta}^4}(\bar{\alpha} - 1) \tag{C4b}$$

$$P_{043} = 0 \tag{C4c}$$

$$P_{044} = \frac{\bar{\alpha}^2}{\bar{\eta}^4(1+\bar{\eta})}\left[\bar{q}_2(\bar{\alpha} - 1) + \bar{\eta}(1+\bar{\eta})\sin\bar{\theta}\right] \tag{C4d}$$

$$P_{045} = -\frac{\bar{\alpha}^2}{\bar{\eta}^4(1+\bar{\eta})}\left[\bar{q}_2\bar{\beta} + (1+\bar{\eta})\cos\bar{\theta}\right] \tag{C4e}$$

$$P_{046} = 0 \tag{C4f}$$

$$P_{051} = -\frac{3\bar{\alpha}}{2\bar{\eta}} \tag{C5a}$$

$$P_{052} = -\frac{\bar{\alpha}^2\bar{\beta}}{\bar{\eta}^4} \tag{C5b}$$

$$P_{053} = 0 \tag{C5c}$$

$$P_{054} = \frac{3\bar{q}_1}{\bar{\eta}^3}\bar{\alpha} + \frac{2}{\bar{\eta}}\cos\bar{\theta} - \frac{\bar{\beta}}{\bar{\eta}^3}\left[\frac{\bar{q}_2}{\bar{\eta}(1+\bar{\eta})}\bar{\alpha}^2 + (\bar{\alpha}+1)\,\sin\bar{\theta} + \bar{q}_2\right] \tag{C5d}$$

$$P_{055} = \frac{3\bar{q}_2}{\bar{\eta}^3}\bar{\alpha} + \frac{2}{\bar{\eta}}\sin\bar{\theta} + \frac{\bar{\beta}}{\bar{\eta}^3}\left[\frac{\bar{q}_1}{\bar{\eta}(1+\bar{\eta})}\bar{\alpha}^2 + (\bar{\alpha}+1)\,\cos\bar{\theta} + \bar{q}_1\right] \tag{C5e}$$

$$P_{056} = \frac{\bar{\beta}}{\bar{\eta}} \cos \bar{i} \tag{C5f}$$

$$P_{061} = 0 \tag{C6a}$$
$$P_{062} = 0 \tag{C6b}$$
$$P_{063} = \frac{1}{\bar{\eta}}(\bar{q}_1 + \cos\bar{\theta}) \tag{C6c}$$
$$P_{064} = 0 \tag{C6d}$$
$$P_{065} = 0 \tag{C6e}$$
$$P_{066} = \frac{1}{\bar{\eta}}(\bar{q}_2 + \sin\bar{\theta}) \sin \bar{i} \tag{C6f}$$

$$P_{J11} = -\frac{3}{4}\bar{\eta}(1 - 3\cos^2 \bar{i}) - \frac{\bar{\eta}^2}{4}\frac{(1+2\bar{\eta})}{(1+\bar{\eta})^2}({\bar{q}_1}^2 - {\bar{q}_2}^2) \sin^2 \bar{i} \tag{C7a}$$
$$P_{J12} = 0 \tag{C7b}$$
$$P_{J13} = \frac{9}{2}\bar{\eta} \sin \bar{i} \, \cos \bar{i} + \frac{\bar{\eta}^2}{2}\frac{(1+2\bar{\eta})}{(1+\bar{\eta})^2}({\bar{q}_1}^2 - {\bar{q}_2}^2) \sin \bar{i} \, \cos \bar{i} \tag{C7c}$$
$$P_{J14} = \frac{9\bar{q}_1}{4\bar{\eta}}(1 - 3\cos^2 \bar{i}) - \frac{\bar{q}_1 \sin^2 \bar{i}}{(1+\bar{\eta})^2}\left[\frac{1 + 3\bar{\eta} + 3\bar{\eta}^2}{(1+\bar{\eta})}{\bar{q}_2}^2 - \frac{1}{2}(1 + 2\eta + \bar{\eta}^2 - \bar{\eta}^3)\right] \tag{C7d}$$
$$P_{J15} = \frac{9\bar{q}_2}{4\bar{\eta}}(1 - 3\cos^2 \bar{i}) + \frac{\bar{q}_2 \sin^2 \bar{i}}{(1+\bar{\eta})^2}\left[\frac{1 + 3\bar{\eta} + 3\bar{\eta}^2}{(1+\bar{\eta})}{\bar{q}_1}^2 - \frac{1}{2}(1 + 2\eta + \bar{\eta}^2 - \bar{\eta}^3)\right] \tag{C7e}$$
$$P_{J16} = 0 \tag{C7f}$$

$$P_{J21} = \frac{9}{4}\bar{q}_1\bar{q}_2 \sin^2 \bar{i} \tag{C8a}$$
$$P_{J22} = \frac{3}{8}\left(3 - \bar{\eta}^2\right)(1 - 3\cos^2 \bar{i}) - \frac{\bar{\eta}}{4}\frac{(1+2\bar{\eta})}{(1+\bar{\eta})^2}({\bar{q}_1}^2 - {\bar{q}_2}^2) \sin^2 \bar{i} \tag{C8b}$$
$$P_{J23} = -\frac{\bar{q}_1\bar{q}_2}{(1+\bar{\eta})^2}\left[3(1+2\bar{\eta}) + 2\bar{\eta}^2(1-\bar{\eta})\right] \sin \bar{i} \, \cos \bar{i} \tag{C8c}$$
$$P_{J24} = -\frac{\bar{q}_1^2\bar{q}_2}{4(1+\bar{\eta})^3\bar{\eta}^2}(18 + 54\bar{\eta} + 51\bar{\eta}^2 + 11\bar{\eta}^3 - 6\bar{\eta}^4) \sin^2 \bar{i}$$

$$-\frac{\bar{q}_2}{4(1+\bar{\eta})}(9+\bar{\eta}+2\bar{\eta}^2)\cos^2\bar{i}-\frac{\bar{\eta}(1-\bar{\eta})\bar{q}_2}{2(1+\bar{\eta})} \tag{C8d}$$

$$P_{J25}=-\frac{\bar{q}_2^2\bar{q}_1}{4(1+\bar{\eta})^3\bar{\eta}^2}(18+54\bar{\eta}+51\bar{\eta}^2+11\bar{\eta}^3-6\bar{\eta}^4)\sin^2\bar{i}$$
$$+\frac{\bar{q}_1}{2(1+\bar{\eta})}(9+4\bar{\eta}+\bar{\eta}^2)\cos^2\bar{i}-\frac{(9+5\bar{\eta}-2\bar{\eta}^2)\bar{q}_1}{4(1+\bar{\eta})} \tag{C8e}$$

$$P_{J26}=\frac{3\bar{\eta}}{4}(1-3\cos^2\bar{i})\cos\bar{i}+\frac{(3+6\bar{\eta}+\bar{\eta}^2-4\bar{\eta}^3)}{8(1+\bar{\eta})^2}(\bar{q}_1^2-\bar{q}_2^2)\sin^2\bar{i}\,\cos\bar{i} \tag{C8f}$$

$$P_{J31}=\frac{3\bar{q}_2}{4}\frac{(1+6\bar{\eta}+3\bar{\eta}^2)}{(1+\bar{\eta})}\sin\bar{i}\,\cos\bar{i} \tag{C9a}$$

$$P_{J32}=\frac{9\bar{q}_1}{4}\sin\bar{i}\,\cos\bar{i} \tag{C9b}$$

$$P_{J33}=\frac{\bar{q}_1^2\bar{q}_2}{4(1+\bar{\eta}^3)}\left[(3+9\bar{\eta}+8\bar{\eta}^2)\cos^2\bar{i}-2\bar{\eta}^2(1+3\bar{\eta})\right] \tag{C9c}$$
$$-\frac{\bar{q}_2}{8(1+\bar{\eta})^2}\left[(6+9\bar{\eta}-10\bar{\eta}^2-23\bar{\eta}^3-14\bar{\eta}^4)\cos^2\bar{i}+(3+15\bar{\eta}+17\bar{\eta}^2+5\bar{\eta}^3-6\bar{\eta}^4)\right]$$

$$P_{J34}=\frac{3\bar{q}_1^2}{2\bar{\eta}(1+\bar{\eta})}\sin\bar{i}\,\cos\bar{i}-\frac{3\bar{q}_1\bar{q}_2}{2\bar{\eta}^2(1+\bar{\eta})}(1+6\bar{\eta}+2\bar{\eta}^2-\bar{\eta}^3)-\frac{3}{2\bar{\eta}}\sin\bar{i}\,\cos\bar{i} \tag{C9d}$$

$$P_{J35}=\frac{3\bar{q}_1\bar{q}_2}{2\bar{\eta}(1+\bar{\eta})}\sin\bar{i}\,\cos\bar{i}-\frac{3\bar{q}_2^2}{2\bar{\eta}^2(1+\bar{\eta})}(1+6\bar{\eta}+2\bar{\eta}^2-\bar{\eta}^3)-\frac{3}{2}(2-\bar{\eta}^2)\sin\bar{i}\,\cos\bar{i} \tag{C9e}$$

$$P_{J36}=\frac{\bar{\eta}\bar{q}_1}{4(1+\bar{\eta})^2}\left[3(1+2\bar{\eta})+2\eta^2(2+\eta)\right](1-3\cos^2\bar{i})\,\sin\bar{i}$$
$$+\frac{(1-\bar{\eta})}{8(1+\bar{\eta})^2}(3+9\bar{\eta}+8\bar{\eta}^2)(\bar{q}_1^2-\bar{q}_2^2)\sin^2\bar{i}\,\cos\bar{i}$$
$$+\frac{\bar{\eta}^2\bar{q}_1}{4(1+\bar{\eta})^2}\left[\frac{2(3+\bar{\eta})}{(1+\bar{\eta})}\bar{q}_2^2-(1+2\bar{\eta}-\bar{\eta}^2)\right]\sin^3\bar{i} \tag{C9f}$$

$$P_{J41}=P_{J42}=P_{J43}=P_{J44}=P_{J45}=P_{J46}=0 \tag{C10}$$

$$P_{J51}=-\frac{3\bar{\eta}}{4}(4-\bar{\eta})$$
$$-\left[\frac{3\eta}{4}\frac{(1+2\bar{\eta})}{(1+\bar{\eta})^2}{\bar{q}_2}^2-\frac{3\bar{\eta}}{8(1+\bar{\eta})}(13+10\bar{\eta}-5\bar{\eta}^2)\right]\sin^2\bar{i} \tag{C11a}$$

$$P_{J52}=0 \tag{C11b}$$

$$P_{J53}=-3\bar{\eta}(2+\bar{\eta})\sin\bar{i}\,\cos\bar{i}-\frac{3}{4}(3-\bar{\eta}^2)\sin\bar{i}\,\cos\bar{i} \tag{C11c}$$

$$P_{J54} = -\frac{\bar{q}_1}{4\bar{\eta}(1+\bar{\eta})}(12 + 17\bar{\eta} + 7\bar{\eta}^2)(1 - 3\cos^2\bar{i}) \tag{C11d}$$

$$P_{J55} = -\frac{\bar{q}_2}{4\bar{\eta}(1+\bar{\eta})}(12 + 17\bar{\eta} + 7\bar{\eta}^2)(1 - 3\cos^2\bar{i}) \tag{C11e}$$

$$P_{J56} = 0 \tag{C11f}$$

$$P_{J61} = \frac{9\bar{q}_1}{2}\sin\bar{i}\,\cos\bar{i} \tag{C12a}$$

$$P_{J62} = 0 \tag{C12b}$$

$$P_{J63} = \frac{9\bar{q}_1}{8}(3 - 7\cos^2\bar{i}) \tag{C12c}$$

$$P_{J64} = -\frac{9\bar{q}_1^2}{\bar{\eta}^2}\sin\bar{i}\,\cos\bar{i} \tag{C12d}$$

$$P_{J65} = -\frac{9\bar{q}_1\bar{q}_2}{\bar{\eta}^2}\sin\bar{i}\,\cos\bar{i} \tag{C12e}$$

$$P_{J66} = \frac{9\bar{q}_2}{8}(1 - 5\cos^2\bar{i})\sin\bar{i} \tag{C12f}$$

References

[1] Hill, G. W., "Researches in the Lunar Theory," *American Journal of Mathematics*, Vol. 1, No. 1, 1878, pp. 5–26.

[2] Clohessy, W. H. and Wiltshire, R. S., "Terminal Guidance System for Satellite Rendezvous," *Journal of the Aerospace Sciences*, Vol. 27, September 1960, pp. 653–658, 674.

[3] Lawden, D. F., *Optimal Trajectories for Space Navigation*, Butterworths, London, UK, 2nd ed., 1963.

[4] Tschauner, J. F. A. and Hempel, P. R., "Rendezvous zu einemin Elliptischer Bahn umlaufenden Ziel," *Astronautica Acta*, Vol. 11, No. 2, 1965, pp. 104–109.

[5] Carter, T. E., "State Transition Matrices for Terminal Rendezvous Studies: Brief Survey and New Examples," *Journal of Guidance, Control, and Dynamics*, Vol. 21, No. 1, January-February 1998, pp. 148–155.

[6] Gim, D.-W. and Alfriend, K. T., "State Transition Matrix of Relative Motion for the Perturbed Noncircular Reference," *Journal of Guidance, Control, and Dynamics*, Vol. 26, No. 6, November-December 2003, pp. 956–971.

[7] Gim, D.-W. and Alfriend, K. T., "Satellite Relative Motion using Differential Equinoctial Elements," *Celestial Mechanics and Dynamical Astronomy*, Vol. 92, No. 4, August

2005, pp. 295–336.

[8] Kasdin, N. J., Gurfil, P., and Kolemen, E., "Canonical Modelling of Relative Spacecraft Motion Via Epicyclic Orbital Elements," *Celestial Mechanics and Dynamical Astronomy*, Vol. 92, No. 4, August 2005, pp. 337–370.

[9] Gurfil, P., "Generalized Solutions for Relative Spacecraft Orbits Under Arbitrary Perturbations," *Acta Astronautica*, Vol. 60, No. 2, January 2007, pp. 61–78.

[10] Alfriend, K. T., Yan, H., and Vadali, S. R., "Nonlinear Considerations in Satellite Formation Flying," *AIAA/AAS Astrodynamics Specialist Conference*, Monterey, CA, 2002, August 2002, AIAA-2002-4741.

[11] Sengupta, P., Vadali, S. R., and Alfriend, K. T., "Second-Order State Transition for Relative Motion near Perturbed, Elliptic Orbits," *Celestial Mechanics and Dynamical Astronomy*, Vol. 97, No. 2, February 2007, pp. 101–129.

[12] Vadali, S. R., Vaddi, S. S., and Alfriend, K. T., "An Intelligent Control Concept for Formation Flying Satellites," *International Journal of Robust and Nonlinear Control*, Vol. 12, 2002, pp. 97–115.

[13] Schaub, H. and Alfriend, K. T., "J_2 Invariant Relative Orbits for Formation Flying," *Celestial Mechanics and Dynamical Astronomy*, Vol. 79, No. 2, February 2001, pp. 77–95.

[14] Garrison, J. L., Gardner, T. G., and Axelrad, P., "Relative Motion in Highly Elliptical Orbits," *Advances in the Astronautical Sciences*, Vol. 89, No. 2, February 1995, pp. 1359–1376, also Paper AAS 95-194 of the AAS/AIAA Space Flight Mechanics Meeting.

[15] Broucke, R. A., "Solution of the Elliptic Rendezvous Problem with the Time as Independent Variable," *Journal of Guidance, Control, and Dynamics*, Vol. 26, No. 4, July-August 2003, pp. 615–621.

[16] Battin, R. H., *An Introduction to the Mathematics and Methods of Astrodynamics*, AIAA Education Series, American Institute of Aeronautics and Astronautics, Inc., Reston, VA, revised ed., 1999.

[17] Broucke, R. A. and Cefola, P. J., "On the Equinoctial Orbit Elements," *Celestial Mechanics*, Vol. 5, 1972, pp. 303–310.

[18] Kaula, W. M., *Theory of Satellite Geodesy*, Dover Publications, Inc., Mineola, NY, 2000.

[19] Brouwer, D., "Solution of the Problem of Artificial Satellite Theory without Drag," *The Astronomical Journal*, Vol. 64, November 1959, pp. 378–397.

[20] Kozai, Y., "The Motion of a Close Earth Satellite," *The Astronomical Journal*, Vol. 64, November 1959, pp. 367–377.

[21] Smith, O. K., "Computation of Coordinates from Brouwer's Solution of the Artificial

Satellite Problem," *The Astronomical Journal*, Vol. 66, No. 7, September 1961, pp. 359–360.

[22] Kozai, Y., "Note on the Motion of a Close Earth Satellite with a Small Eccentricity," *The Astronomical Journal*, Vol. 66, No. 3, April 1961, pp. 132–133.

[23] Lyddane, R. H., "Small Eccentricities or Inclinations in the Brouwer Theory of the Artificial Satellite," *The Astronomical Journal*, Vol. 68, No. 8, October 1963, pp. 555–558.

[24] Aksnes, K., "On the Use of Hill's Variables in Artificial Satellite Theory; Brouwer's Theory," *Astronomy & Astrophysics*, Vol. 17, 1972, pp. 70–75.

[25] Hoots, F. R., "Reformulation of the Brouwer Geopotential Theory for Improved Computational Efficiency," *Celestial Mechanics*, Vol. 24, No. 4, August 1981, pp. 367–375.

[26] Déprit, A. and Rom, A., "The Main Problem of Artificial Satellite Theory for Small and Moderate Eccentricities," *Celestial Mechanics*, Vol. 2, No. 2, July 1970, pp. 166–206.

[27] Aksnes, K., "A Note on 'The Main Problem of Artificial Satellite Theory for Small Eccentricities, By A. Déprit and A. Rom, 1970," *Celestial Mechanics*, Vol. 4, No. 1, September 1971, pp. 119–121.

[28] Déprit, A., "The Main Problem of Artificial Satellites to Order Four," *Journal of Guidance, Control, and Dynamics*, Vol. 4, No. 2, March-April 1981, pp. 201–206.

[29] Coffey, S. L. and Déprit, A., "Third-Order Solution to the Main Problem of Satellite Theory," *Journal of Guidance, Control, and Dynamics*, Vol. 5, No. 4, July-August 1982, pp. 366–371.

[30] Kechichian, J. A., "Motion in General Elliptic Orbit with Respect to a Dragging and Precessing Coordinate Frame," *The Journal of the Astronautical Sciences*, Vol. 46, No. 1, January-March 1998, pp. 25–46.

[31] Schweigart, S. A. and Sedwick, R. J., "High-Fidelity Linearized J_2 Model for Satellite Formation Flight," *Journal of Guidance, Control, and Dynamics*, Vol. 25, No. 6, November-December 2002, pp. 1073–1080.

[32] Yan, H., Sengupta, P., Vadali, S. R., and Alfriend, K. T., "Development of a State Transition Matrix for Relative Motion Using the Unit Sphere Approach," *Advances in the Astronautical Sciences*, Vol. 119, No. 1, February 2004, pp. 935–946, also Paper AAS 04-163 of the AAS/AIAA Space Flight Mechanics Meeting.

[33] Vadali, S. R., "An Analytical Solution for Relative Motion of Satellites," *5th Dynamics and Control of Systems and Structures in Space Conference*, Cranfield University, Cranfield, UK, July 2002.

[34] Junkins, J. L. and Turner, J. D., "On the Analogy Between Orbital Dynamics and Rigid Body Dynamics," *The Journal of the Astronautical Sciences*, Vol. 27, No. 4, October-

December 1979, pp. 345–358.

[35] Born, G. H., Goldstein, D. B., and Thompson, B., "An Analytical Theory for Orbit Determination," *The Journal of the Astronautical Sciences*, Vol. 49, No. 2, April-June 2001, pp. 345–361.

[36] Hoots, F. R., "Theory of Motion of an artificial Earth Satellite," *Celestial Mechanics*, Vol. 23, No. 4, April 1981, pp. 307–363.

[37] Vallado, D. A., *Fundamentals of Astrodynamics and Applications*, Microcosm, Inc., El Segundo, CA, 2nd ed., 2001.

[38] Vadali, S. R., Vaddi, S. S., and Alfriend, K. T., "A New Concept for Controlling Formation Flying Satellite Constellations," *Advances in the Astronautical Sciences*, Vol. 108, No. 2, February 2001, pp. 1631–1648, also Paper AAS 01-218 of the AAS/AIAA Space Flight Mechanics Meeting.

[39] Sengupta, P. and Vadali, S. R., "Formation Design and Geometry for Keplerian Elliptic Orbits with Arbitrary Eccentricity," *Journal of Guidance, Control, and Dynamics*, Vol. 30, No. 4, July-August 2007, pp. 951–962.

[40] Vaddi, S. S., Vadali, S. R., and Alfriend, K. T., "Formation Flying: Accommodating Nonlinearity and Eccentricity Perturbations," *Journal of Guidance, Control, and Dynamics*, Vol. 26, No. 2, March-April 2003, pp. 214–223.

[41] Richardson, D. L. and Mitchell, J. W., "A Third-Order Analytical Solution for Relative Motion with a Circular Reference Orbit," *The Journal of the Astronautical Sciences*, Vol. 51, No. 1, January-March 2003, pp. 1–12.

[42] Sengupta, P., Sharma, R., and Vadali, S. R., "Periodic Relative Motion Near a Keplerian Elliptic Orbit with Nonlinear Differential Gravity," *Journal of Guidance, Control, and Dynamics*, Vol. 29, No. 5, September-October 2006, pp. 1110–1121.

[43] Lewis, F. L. and Syrmos, V. L., *Optimal Control*, John Wiley & Sons, Inc., New York, NY, 2nd ed., 1995.

List of Figure Captions

Figure 1: Osculating, Mean and Average Error: Radial
a): Position
b): Velocity

Figure 2: Osculating, Mean and Average Error: Along-Track
a): Position
b): Velocity

Figure 3: Osculating, Mean and Average Error: Out-of-Plane
a): Position
b): Velocity

Figure 4: Control Effort for Formation-Keeping

Figure 5: Error in Relative Position

Figure 6: Cost for Formation-Keeping

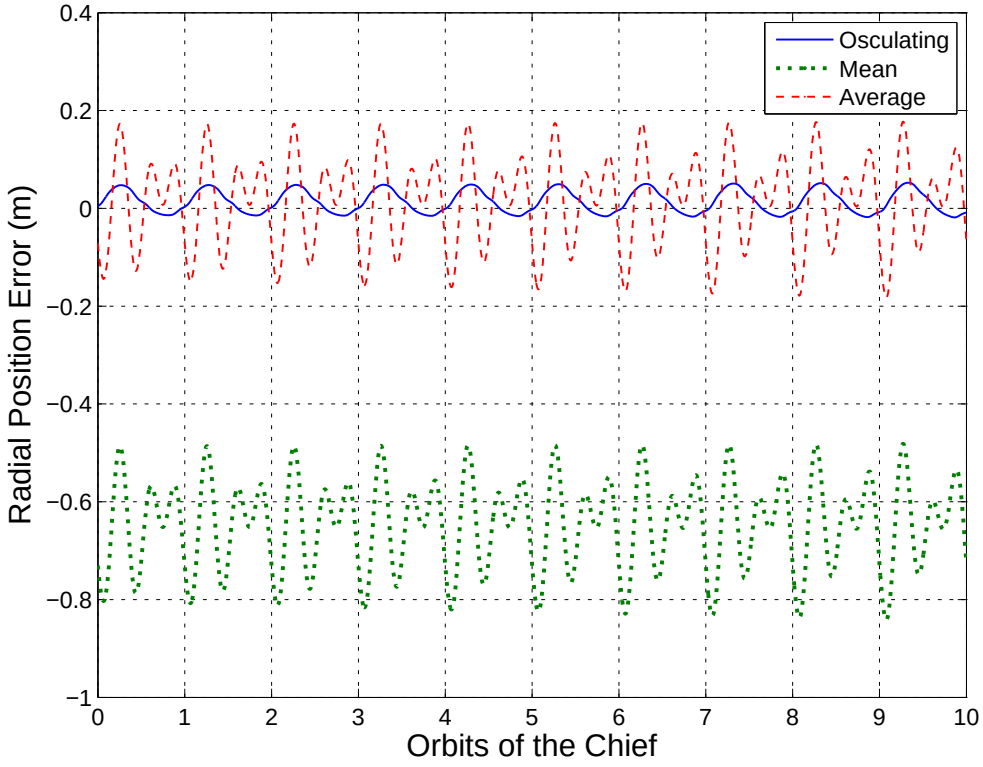

Position

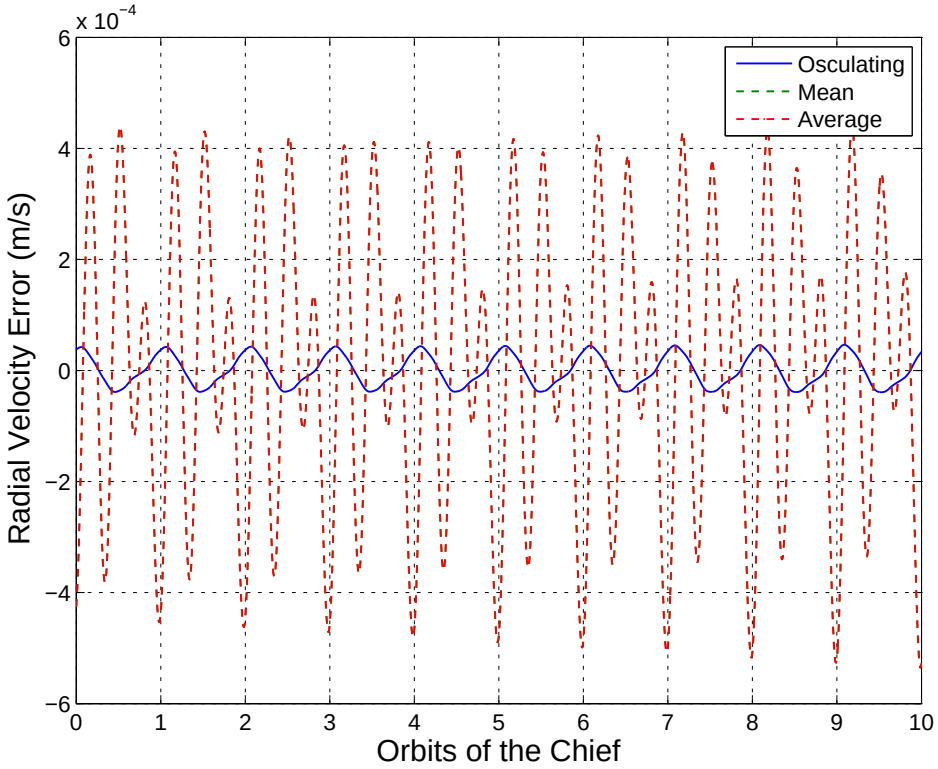

Velocity

FIGURE 1:

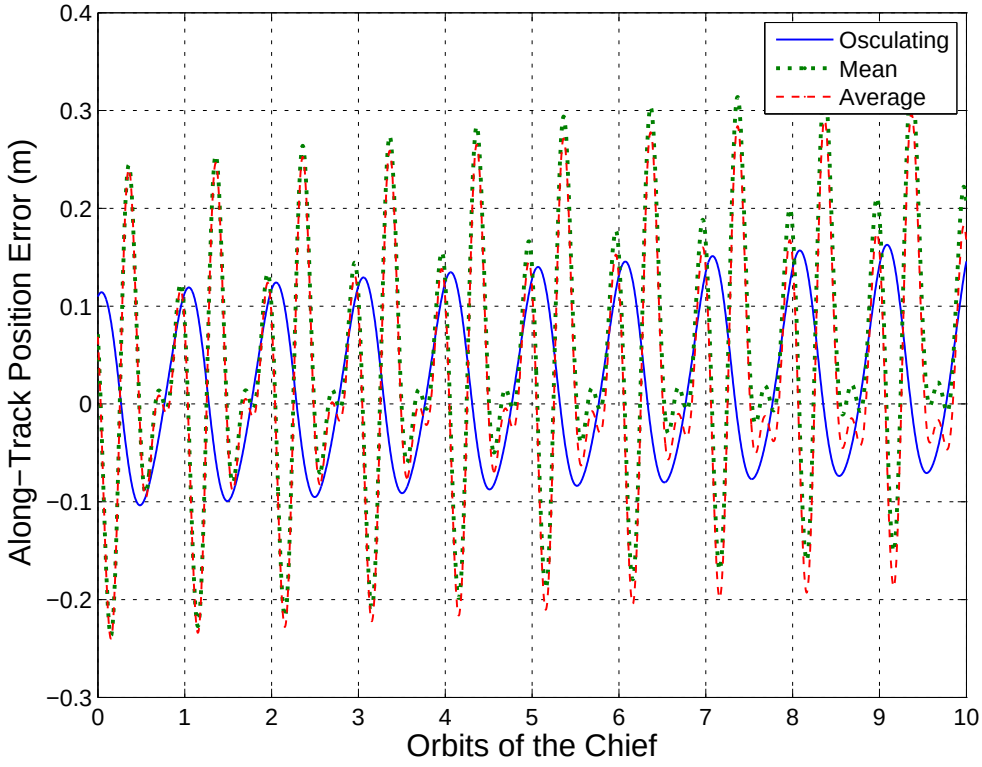

Position

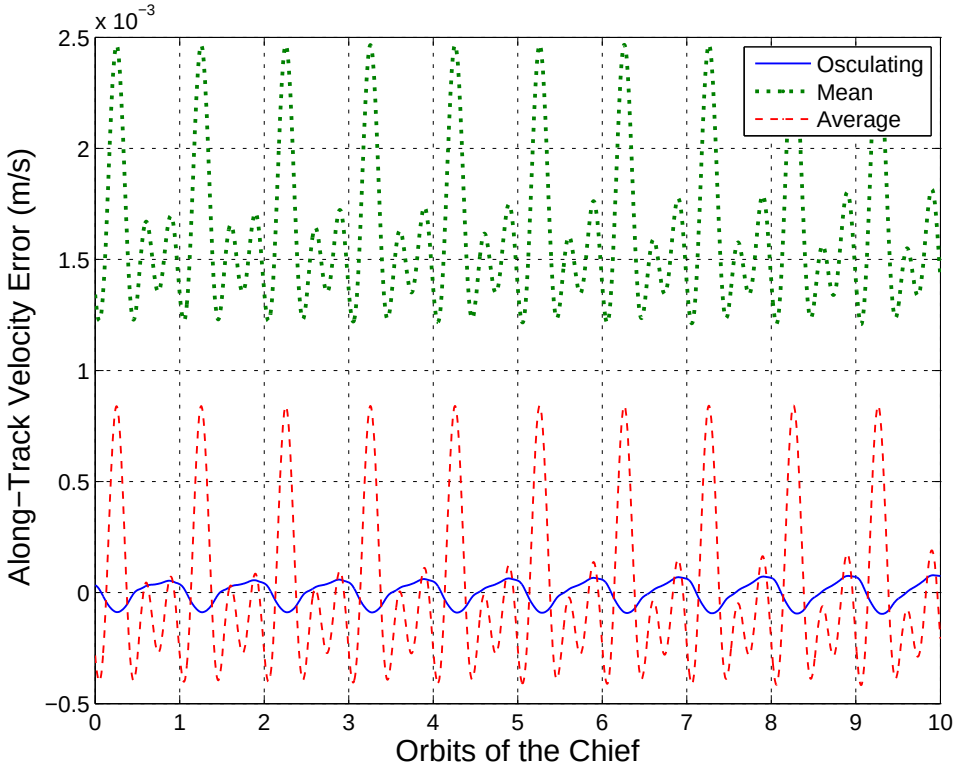

Velocity

FIGURE 2:

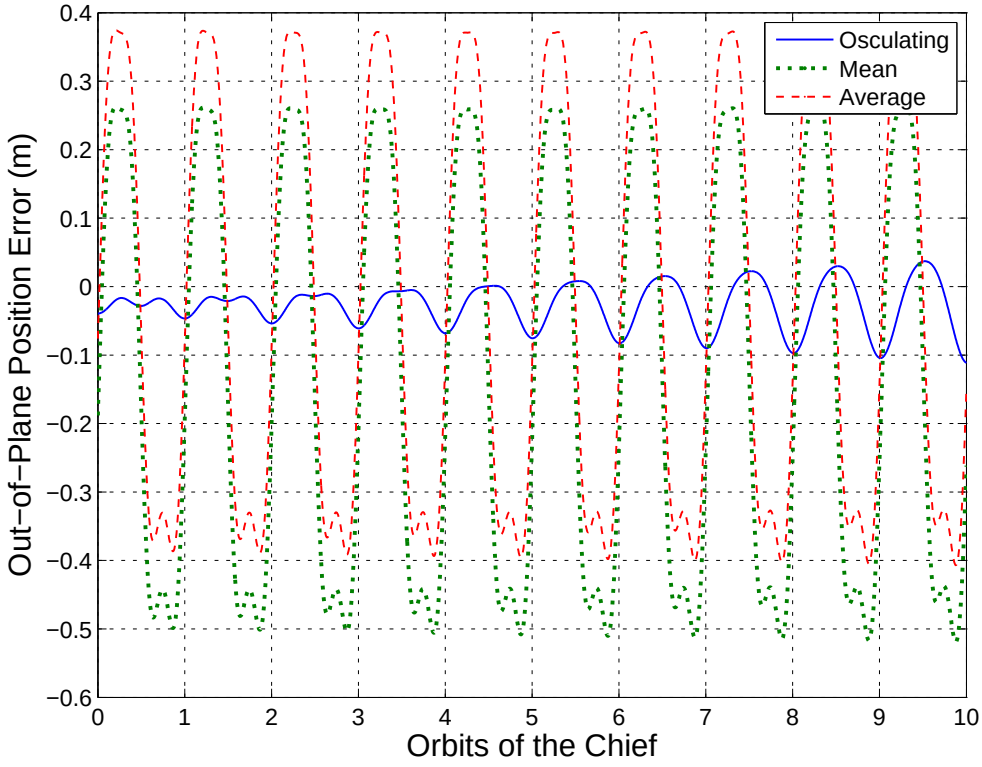

Position

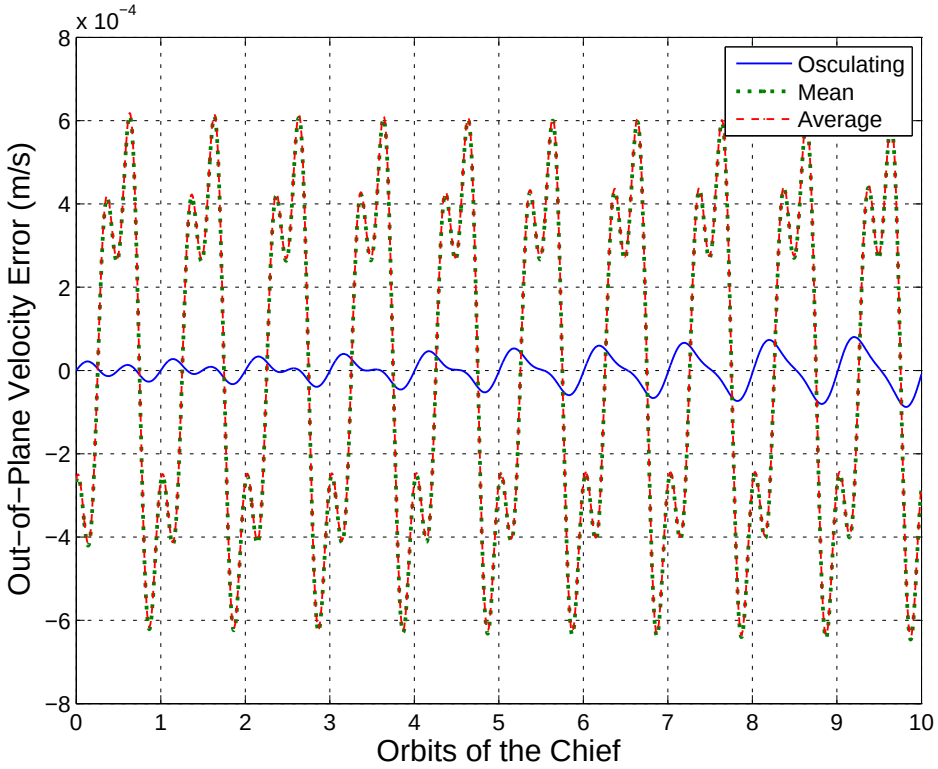

Velocity

FIGURE 3:

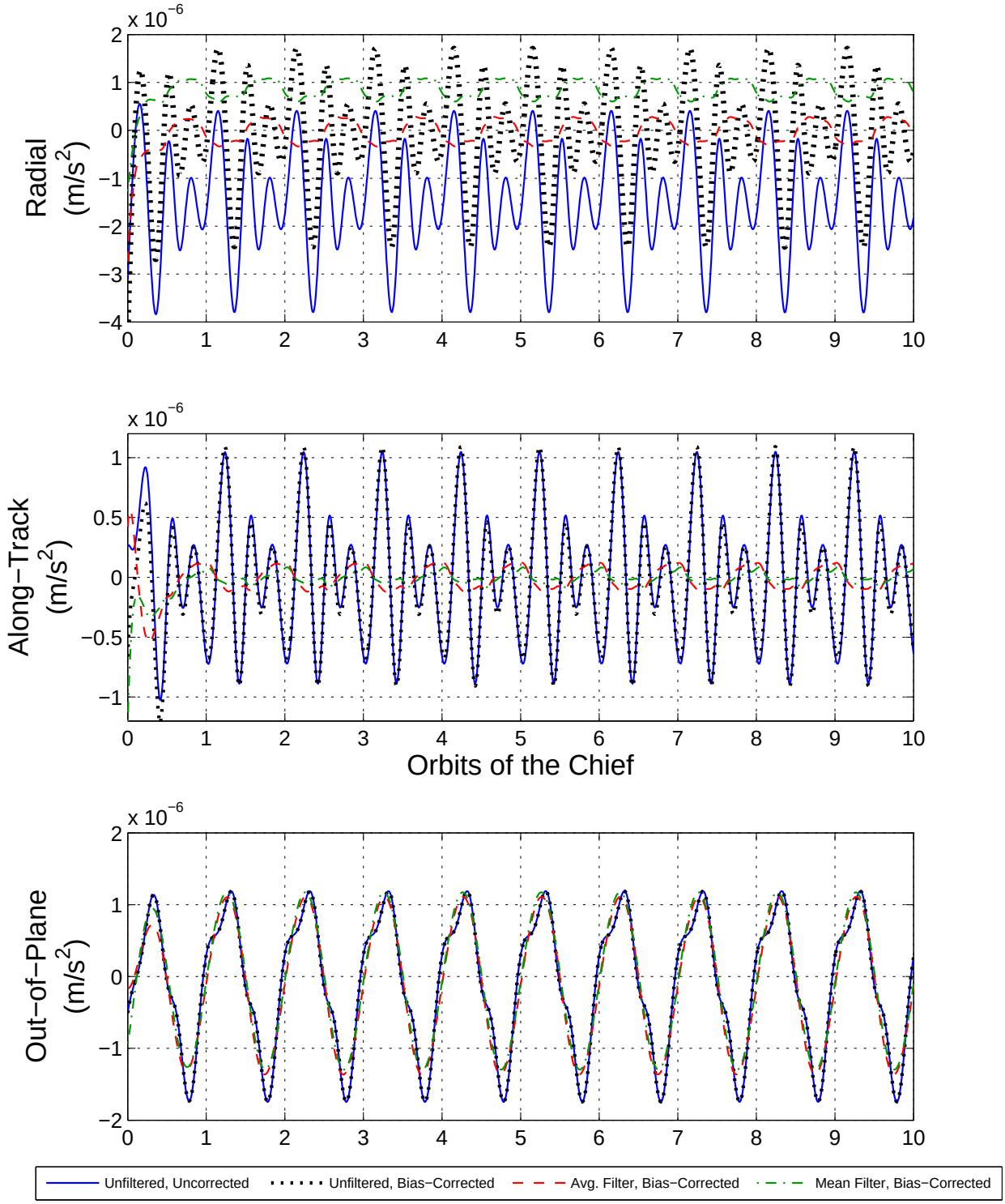
x 10^−6
Radial (m/s^2)
Along−Track (m/s^2)
Out−of−Plane (m/s^2)
Orbits of the Chief
Unfiltered, Uncorrected
Unfiltered, Bias−Corrected
Avg. Filter, Bias−Corrected
Mean Filter, Bias−Corrected

FIGURE 4:

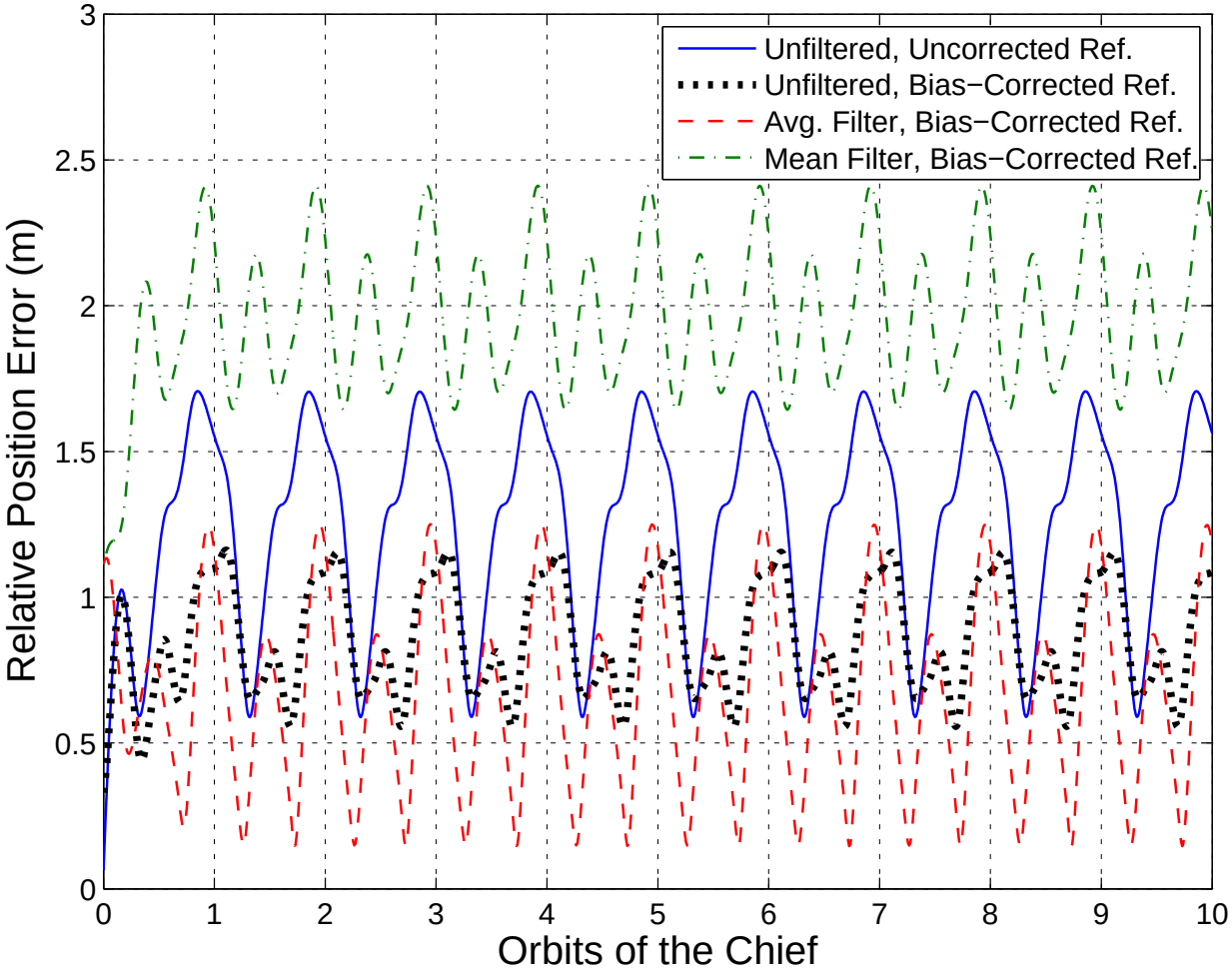
Unfiltered, Uncorrected Ref.
Unfiltered, Bias−Corrected Ref.
Avg. Filter, Bias−Corrected Ref.
Mean Filter, Bias−Corrected Ref.
Relative Position Error (m)
Orbits of the Chief
0
0.5
1
1.5
2
2.5
3
0
1
2
3
4
5
6
7
8
9
10

FIGURE 5:

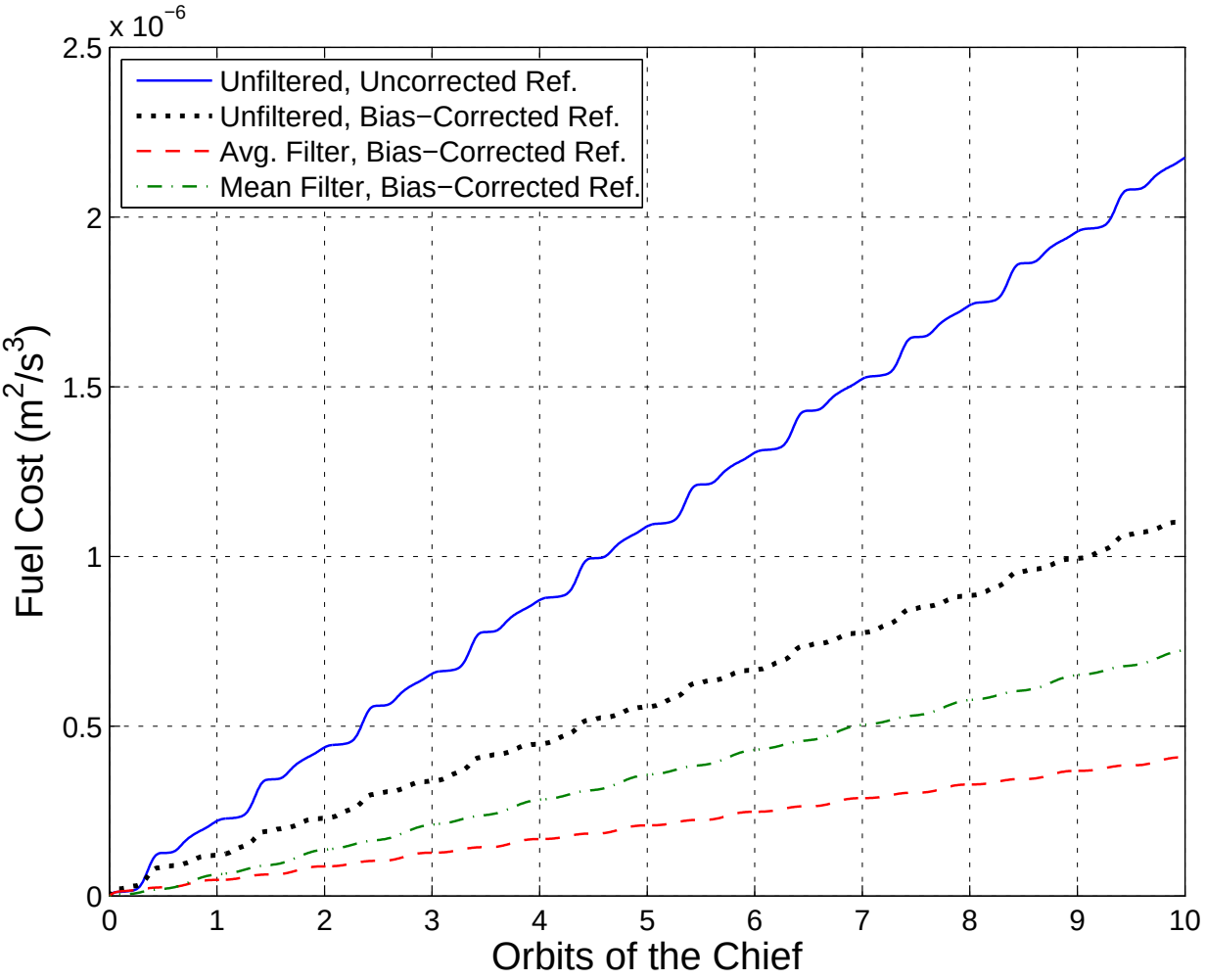
x 10^−6
2.5
2
1.5
1
0.5
0
Fuel Cost (m^2/s^3)
Unfiltered, Uncorrected Ref.
Unfiltered, Bias−Corrected Ref.
Avg. Filter, Bias−Corrected Ref.
Mean Filter, Bias−Corrected Ref.
0
1
2
3
4
5
6
7
8
9
10
Orbits of the Chief

FIGURE 6: